

# **Samos Island, Part I: metamorphosed and non- metamorphosed nappes, and sedimentary basins**

**Uwe Ring**

Department of Geological Sciences, Canterbury University, Christchurch 8004, New Zealand  
*Email: [uwe.ring@canterbury.ac.nz](mailto:uwe.ring@canterbury.ac.nz)*

**Martin Okrusch**

Institut für Mineralogie, Universität Würzburg, 97074 Würzburg, Germany  
*Email: [okrusch@mail.uni-wuerzburg.de](mailto:okrusch@mail.uni-wuerzburg.de)*

**Thomas Will**

Institut für Mineralogie, Universität Würzburg, 97074 Würzburg, Germany  
*Email: [thomas.will@mail.uni-wuerzburg.de](mailto:thomas.will@mail.uni-wuerzburg.de)*

Keywords: Samos, geological excursion

**Abstract:** This excursion guide is subdivided into two parts: the first deals with aspects of the geologic, tectonic and metamorphic evolution of Samos and the second with the famous fossils of the islands. The first part is accompanied by an itinerary for a 5-day field trip. Chapter 2 does not include a detailed field trip program but contains a map that shows the main sites of the bone beds that contain the world-famous Neogene mammals of Samos.

## Table of Contents

Introduction .....	4
Geology of Samos .....	4
General Architecture of Samos and Important Tectonic Contacts .....	6
Metamorphic History .....	8
Petrography of metabasic rocks of Selçuk nappe .....	8
Petrography of metapelitic rocks of Ampelos nappe .....	8
Petrography of glaucophanites of Agios Nikolaos nappe .....	9
P-T estimates .....	9
Structural History and Deformation/Metamorphism Relationships .....	11
Geomorphology and Holocene Uplift of Northwestern Samos .....	12
Field Trips .....	13
Day 1: Metamorphosed rocks of the Ampelos and Agios Nikolaos nappe and Neogene sediments of Mytilini basin in East and North Samos .....	14
Day 2: Uplifted shorelines, Neogene sediments and volcanics of the Karlovasi basin and met- amorphosed rocks of the Ampelos and nappe in western central Samos .....	18
Day 3: Triassic granite and traverse from Ampelos into Kerketas nappe .....	21
Day 4: Kerketas and Kallithea nappe .....	22
Day 5: South coast .....	24
References .....	26

## Introduction

Samos is not one of the typical Aegean “turtle-back shaped core-complex type” islands as Ios or Mykonos for example. The general structure of Samos is dominated by steep faults and the overall architecture of the islands is best described as a horst. Samos is very rugged and dominated by the sheer cliffs of the 1433 m high Kerkis Mountain in the west (Fig. 1).

**Figure 1. The Kerketas Massif viewed from the SW**



Kerkis Mountain is at 1433 m one of the highest peaks in the central Aegean. The grey coloured marbles in the upper parts of the photographs belong to the Kerketas nappe, which is part of the Basal unit of the Cycladic

nappe stack and interpreted to be correlative to the Tripolitza unit of the External Hellenides. The photograph also shows the presently very rugged topography of Samos Island and Dilek Peninsula on the adjacent western Turkish mainland.

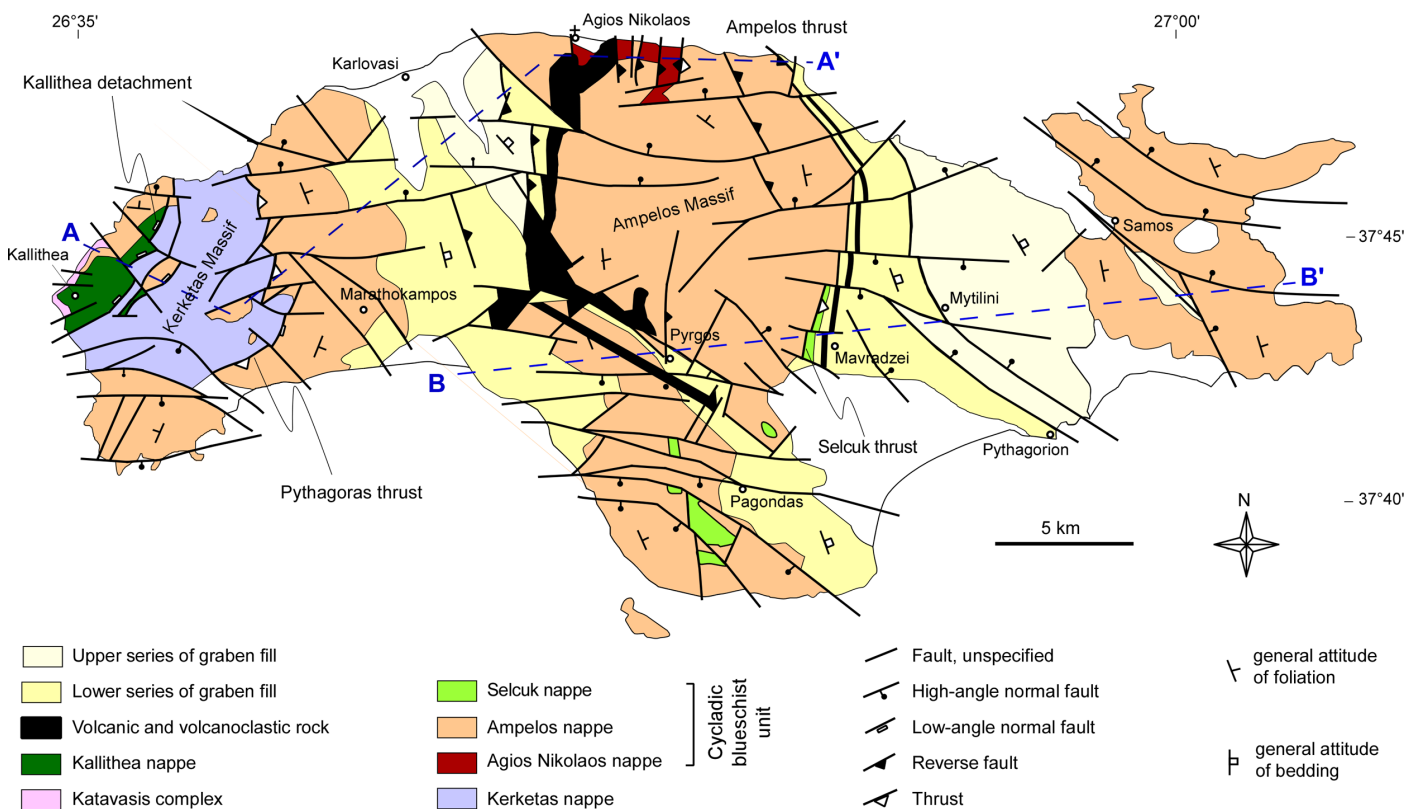
The geology of Samos consists of a number of metamorphosed nappes, one non-metamorphosed nappe and Miocene graben. Because of the quite complicated geology, the island offers a look on an exceptionally complete nappe stack of the Central Hellenides ranging from the high-pressure metamorphosed Basal Unit (as part of the External Hellenides) all the way up to the ophiolitic Sélcuk nappe and the non-metamorphosed Cycladic ophiolite nappe.

However, scientifically Samos became famous for another reason: the island is widely regarded as one of the best localities in the world for Neogene mammalian palaeontology. Up to now about 50,000 specimens have been collected and they are distributed in more than 30 museums and universities in Europe and the USA.

## Geology of Samos

A simplified geological map of Samos Island is shown in Figure 2, the nappe pile is summarised in Table 1, the Neogene basins in Table 2, the entire sequence is schematically depicted in Figure 3 and shown on two cross sections in Figure 4. The nappe stack consists of six major tectonic units, which are described in descending order:

Figure 2. Simplified geological and tectonic map of Samos Island



Map shows major rock units, thrusts and faults (with barbs and ticks on the hanging-wall sides) and representative structural attitudes of rocks. The different nappes are described in Table 1. Lower series of graben fill comprise Basal Conglomerate, Pythagorion and Hora Formations; Upper series of graben fill include Mytilini and Kokkarion Formations (see also Figs 3 and 4 and Table 2). The D<sub>1</sub> Ampelos and Selçuk thrusts are the basal thrusts of the Ampelos and Selçuk nappes, respectively. The D<sub>2</sub> Pythagoras thrust put the Cycladic blueschist unit on top of the Kerketas nappe (the Pythagoras thrust is named after 'Pythagoras Cave' c. 50 m above the thrust plane west of Marathokampos). The Kallithea detachment is a late-D<sub>3</sub> low-angle normal fault. Widespread Middle and mainly Late Miocene volcanic and volcanoclastic rocks occur at the eastern and north-eastern margin of the Karlovasi and Pyrgos graben. Subordinate volcanics also occur at the western side of the Mytilini basin. Numerous reverse (D<sub>4</sub>) and normal (D<sub>5</sub>) faults overprinted all earlier ductile contacts. We interpret the curved D<sub>5</sub> high-angle normal faults to have a listric geometry.

(1) The Kallithea nappe is part of the Cycladic ophiolite nappe of the Upper unit. It consists of peridotite, basalt, Triassic-Jurassic limestone, radiolarite and sandstone (Theodoropoulos 1979). The Katavasis complex consisting of amphibolite-facies schist, marble and amphibolite forms a tectonic block in the Kallithea nappe (Ring et al. 1999a).

(2) The Selçuk nappe is the uppermost nappe of the Cycladic blueschist unit and only exposed in a few patches. It is far more extensively exposed on the westernmost Turkish mainland some 10-20 km to the east of Samos (Gessner et al. this volume). The Selçuk nappe is essentially an ophiolitic mélangé and contains metagabbro, in part in primary contact with serpentinitized peridotite, and mica schist.

(3) The Ampelos nappe is made up of the shelf sequence of the Cycladic blueschist unit and contains marble (with metabauxite lenses), metapelite (including conspicuous chloritoid-kyanite schist), quartzite, glaucophane-epidote schist and greenschist. Detailed work by Ring and co-workers showed that the Ampelos nappe is correlative with the Dilek nappe of adjacent western Turkey (Ring et al. 1999a, b, 2007; Gessner et al. 2001; see also Gessner et al. this volume).

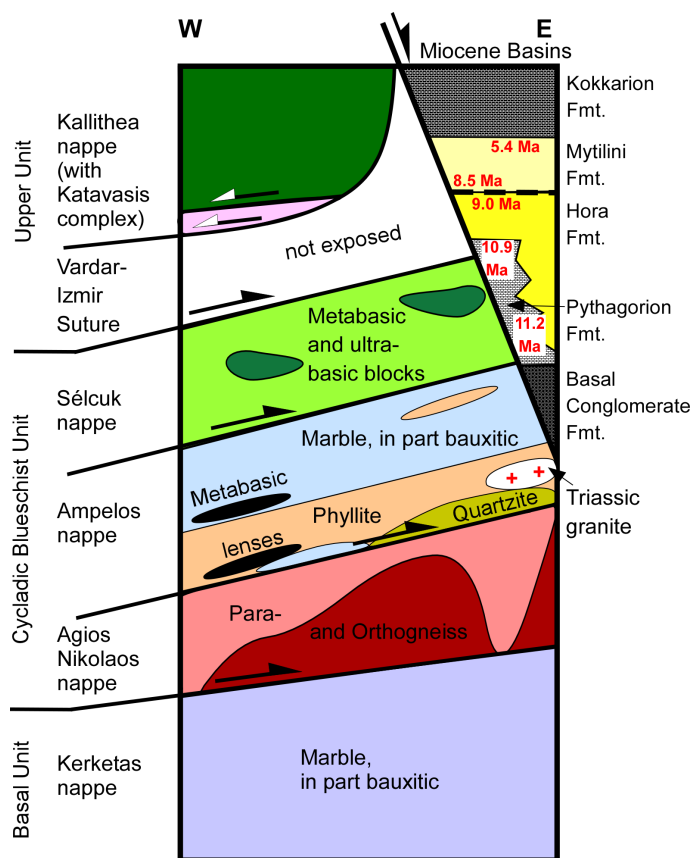
(4) The Agios Nikolaos nappe at the base of the Cycladic blueschist unit is, like the Selçuk nappe, only exposed in a few outcrops at the northern coast between the church of Agios Nikolaos and Konstandinos. It forms part of the Carboniferous and pre(?) Carboniferous basement of the

Cycladic blueschist unit and consists of metagranitic gneiss, garnet-mica schist and dolomitic marble.

(5) The Kerketas nappe of the Basal unit is made up of an at least 1000 m thick succession of monotonous dolomitic marble, the base of which is not exposed (Fig. 1). The Basal unit is generally correlated with the Tripolitza unit of the External Hellenides (Godfriaux 1968).

(6) Molasse-type sediments were deposited in the Miocene and Pliocene in N-, NE- and WNW-oriented Karlovasi, Pyrgos and Mytilini graben, which are filled with fluvial and lacustrine sediments (Table 2, Fig. 3) (note that the sediments of the Mytilini basin and its fossil content is described in more detail in Chapter 2). Above the Basal Conglomerate Formation follows the Pythagorion and Hora Formations. Both formations also laterally interfinger with each other. The sediments of the Hora Formation are thought to have formed in a deeper basin than the limestone of the Pythagorion Formation (Weidmann et al. 1984). A major angular unconformity occurs on top of the Hora Formation. Lacustrine sedimentation is succeeded by fluvial conglomerate of the basal Mytilini Formation (Old Mill Beds sensu Weidmann et al. 1984). Weidmann (1984) showed that in some places the unconformity occurs on top of the Old Mill Beds, whereas in other places it occurs below the Old Mill Beds. This difference might indicate that the unconformity did not occur at the same time in all parts of the basin or it might indicate that the Old Mill beds are time-transgressive.

**Figure 3. Idealized comparative tectonostratigraphic columns of the nappe pile on Samos Island**

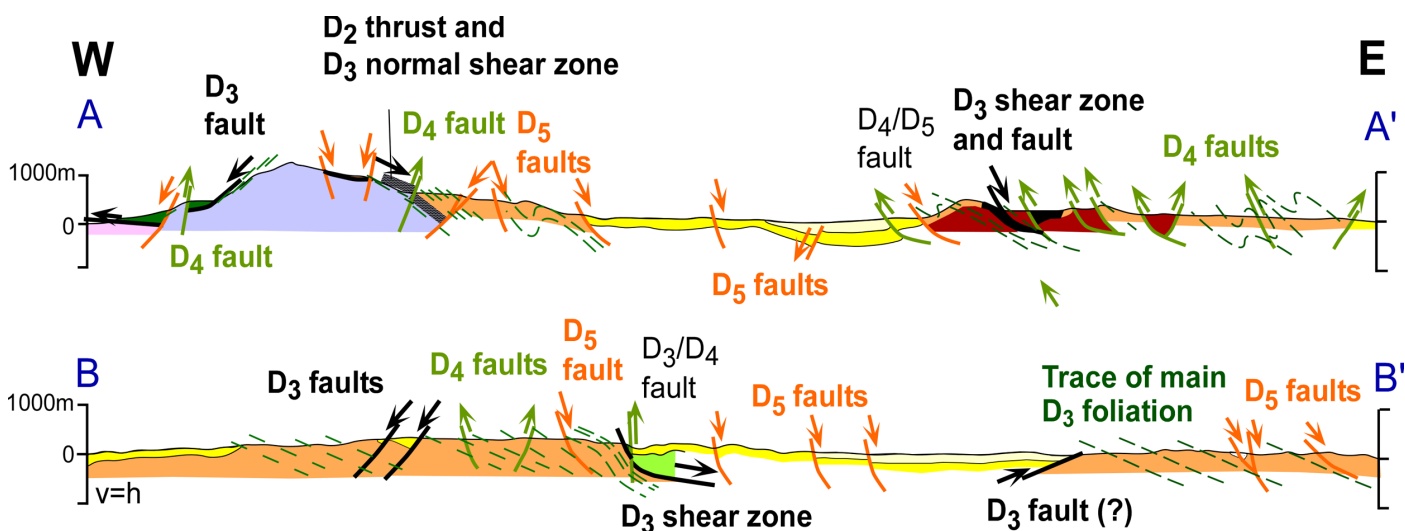


Ar-Ar age data of Weidmann et al. (1984) provide age constraints for sedimentary rocks in Miocene basins.

### General Architecture of Samos and Important Tectonic Contacts

The island of Samos in the Aegean Sea exposes high-pressure metamorphic rocks of the Cycladic blueschist unit which are sandwiched between the mildly blueschist-facies Kerketas nappe below and the overlying non-metamorphic Kallithea nappe. The general architecture of the island is depicted in two generalized cross sections in Figure 4. Overall the nappe pile is dipping to the east.

Figure 4. Serial cross sections



(a) and (b). Serial cross sections A-A' and B-B' through Samos Island showing general architecture of the island (refer to Fig. 2 for transect positions). The trace of the main foliation illustrates the generally E-dipping structure.

The base of the Kerketas nappe is not exposed. At its northern end the dolomite of the Kerketas nappe can be followed from the top of Kerkis Mountain down to the sea. The contact of the Kerketas nappe with the Agios Nikolaos nappe has been excised, either by Eocene out-of-sequence thrusting, and/or subsequent Eocene normal shearing, or Miocene extensional shearing (see below). What is well exposed is the Pythagoras thrust separating the Kerketas nappe from the overlying Ampelos nappe (see field trip stop 3.2 below). Ring and Layer (2003) interpreted  $^{40}\text{Ar}/^{39}\text{Ar}$  phengite ages of ~30-35 Ma to date shear-related phengite recrystallization during thrusting of the Cycladic blueschist unit onto the Kerketas nappe. The Pythagoras thrust was then reactivated as a top-E extensional fault in the Middle Miocene probably associated with the formation of the Middle Miocene basins.

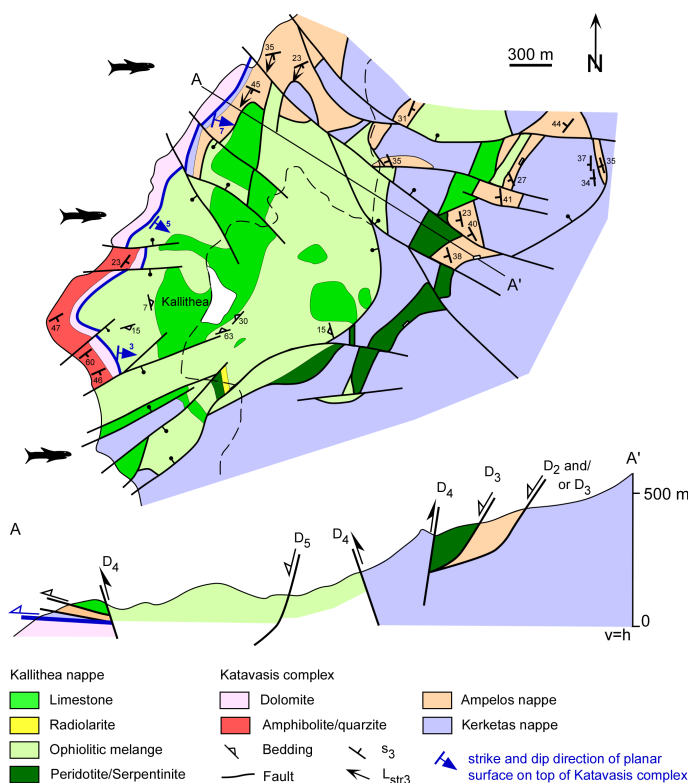
The base of the Agios Nikolaos nappe is nowhere exposed. The upper contact of the Agios Nikolaos nappe is poorly exposed in the northern Ampelos Massif at the central north coast of the island. There is no unambiguous evidence as to whether this contact is a thrust-type or normal shear zone. Ring et al. (2007) speculated that the latest penetrative ductile deformation might be normal and related to the Eocene motion of the Selçuk normal shear zone (see below).

The Selçuk normal shear zone separates the Ampelos nappe from the overlying Selçuk nappe. Rb-Sr dating revealed that the Selçuk normal shear zone was active from

42-32 Ma (Ring et al. 2007). Normal shearing caused extensive retrogression of the high-pressure parageneses in the Selçuk nappe (see below). Normal shearing is a geometric effect facilitating the extrusion of the Ampelos nappe (together with its western Turkish equivalent, the Dilek nappe); it is not related to wholesale crustal extension of the region.

The next major contact in the tectonic sequence is the Kallithea detachment in western Samos. Figure 5 shows a detailed map and cross section of the Kallithea nappe and the Kallithea detachment at its base. Ring et al. (1999a) argued that the detachment was active between 10-8.5 Ma. Subsequent zircon fission-track dating by Stephanie Brichau (published in Kumerics et al. 2005) revealed that the Kallithea detachment, or a splay of it, continued moving until or was reactivated at ~7 Ma (see stop 4.3 below).

Figure 5. Map and cross section



(a) and (b) Detailed map and cross section of Kallithea nappe and adjacent units. The contact between the Katavasis complex and the Kallithea and Kerketas nappes, respectively, is marked by a conspicuous ~50 cm thick dark-grey cataclasite.

The Miocene basins on Samos have a complex architecture and tectonic history. It seems that formation of the basins was related to extensional reactivation of the Pythagoras thrust in the Middle Miocene in a transtensional setting. Ring et al. (1999a) argued that a transtensional scenario might best explain the abrupt lateral facies changes of the Hora and Pythagorion Formations. There is plenty of evidence for folding in the Hora and Pythagorion Formations caused by a short-lived shortening event at  $>8.6$  to  $\sim 9$  Ma (e.g. stop 2.3 below, see also Structural History).

## Metamorphic History

In this section critical rock types of the Selçuk, Ampelos and Agios Nikolaos nappes will be described followed by estimates of P-T conditions of metamorphic events. Details of the metamorphic history are given in Will et al. (1998) and Ring et al. (2007).

## Petrography of metabasic rocks of Selçuk nappe

The Selçuk nappe metagabbros are usually massive, sodic amphibole-bearing rocks; omphacitic pyroxene may be present. Strongly mylonitized metagabbros from the Selçuk normal shear zone contain sodic amphibole and diopside pyroxene, but lack omphacite. Garnet-bearing amphibolites of the Selçuk nappe occur in adjacent western Turkey (Ring et al. 2007).

The massive glaucophane-bearing metagabbros without omphacite are predominantly made up of sodic and calcic amphiboles, epidote, albite and chlorite. In addition, various amounts of biotite, titanite, magnetite, ilmenite and traces of white mica occur. The rocks have a coarse-grained, relic magmatic texture, which was modified during metamorphism. The metamorphic mineral assemblage sodic amphibole-epidote-white mica is ascribed to blueschist-facies metamorphic conditions, and the assemblage calcic to barroisitic amphibole-epidote-chlorite-albite to a subsequent decompression stage.

The massive omphacite-bearing metagabbros also preserve high pressure assemblages. The rocks contain green and colourless hornblende, diopside and omphacitic pyroxene (31-52 mole% jadeite), epidote, chlorite, albite, quartz, and accessory titanite. Generally, these rocks preserve a relic magmatic texture: large, anhedral magmatic green hornblende is rimmed by pale green to colourless actinolite and actinolite-chlorite±titanite intergrowths. Magmatic clinopyroxene is rimmed by green hornblende and, in places, replaced by colourless chlorite. Plagioclase occurs as (i) large poikiloblasts containing fine-grained actinolite, chlorite and epidote and, (ii) as fine-grained recrystallized matrix minerals. Pseudomorphs of paragonite, zoisite and quartz after lawsonite are preserved in some rocks.

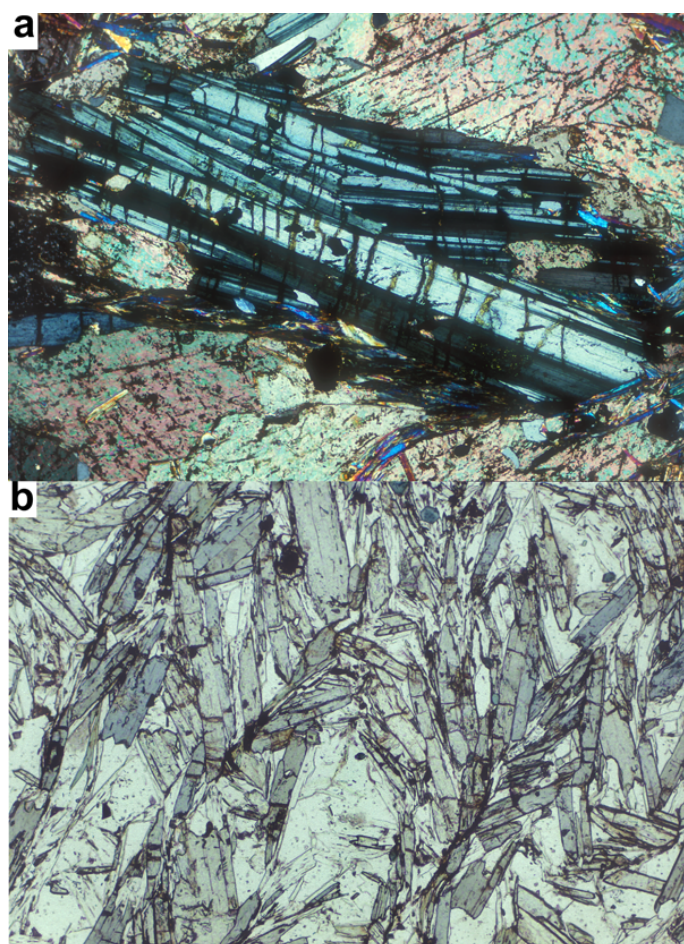
The strongly mylonitized metagabbros contains relicts of magmatic diopside pyroxene and brown, Ti-bearing amphibole. Furthermore green-blue and colourless amphibole, chlorite, albite, epidote and quartz are present. Accessory titanite, biotite and opaque phases, which are generally transformed to leucoxene, occur.

## Petrography of metapelitic rocks of Ampelos nappe

The metapelitic rocks from the Ampelos nappe are strongly foliated, fine-grained rocks. Kyanite and chloritoid are sometimes abundant in metapelitic rocks (Fig. 6).

Up to 0.6 mm large (in diameter) twinned chloritoid poikiloblasts occur in a fine-grained matrix of quartz, phengitic muscovite (3.06 to 3.13 Si per formula unit for 11 oxygens), paragonite and minor chlorite. Zoisite is present in some samples, and Mg-carpholite was found in one sample from Samos by Okrusch (1981). The foliation is defined by white mica and a shape preferred orientation of quartz and wraps around chloritoid. Inclusions in chloritoid are plagioclase, quartz, opaque phases and white mica. Locally, kyanite crystals exhibit undulose extinction, commonly they are surrounded by quartz-filled pressure shadows and contain plagioclase and quartz inclusions.

**Figure 6. Metamorphic assemblages**

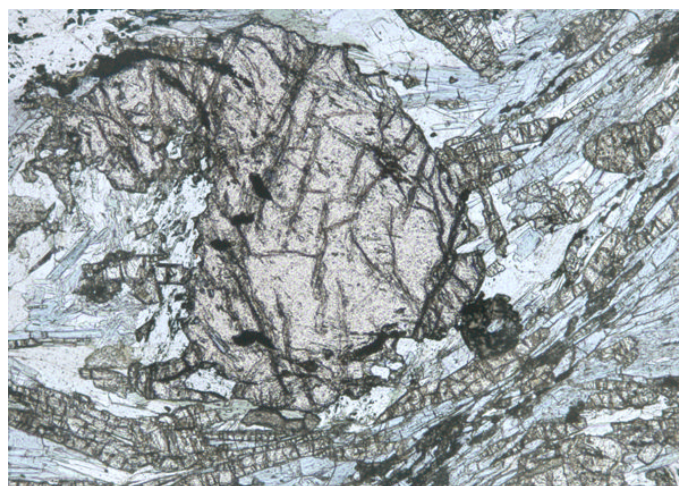


Assemblage chloritoid (blue in different shades) + ankerite + phengite in silicate-ankerite marble, sample Sa91-5, Psili Amos Bay, Eastern Samos (crossed-polarized light, photo width 1.9 mm). (b) Assemblage chloritoid (predominant, light olive green or blue) + chlorite (subordinate, light green) + phengite + quartz in metapelitic schist, sample Sa80-165, Moni Megali Panagias, central Samos (plane-polarized light, photo width 1.25 mm).

### **Petrography of glaucophanites of Agios Nikolaos nappe**

The garnet-bearing glaucophanites of the Agios Nikolaos nappe (field trip stop #1.6) contain varying proportions of sodic and calcic amphiboles, garnet, paragonite, muscovite, zoisite, chlorite, albite, titanite and quartz (Fig. 7). Pseudomorphs of zoisite, quartz and little paragonite after lawsonite are preserved as inclusions in garnet testifying the prograde stability of lawsonite (Will et al. 1998). Calcic amphibole together with, or without, chlorite surrounds sodic amphibole in some cases. Coexisting garnet and sodic amphibole are restricted to the Agios Nikolaos nappe glaucophanites.

**Figure 7. Metamorphic assemblage**

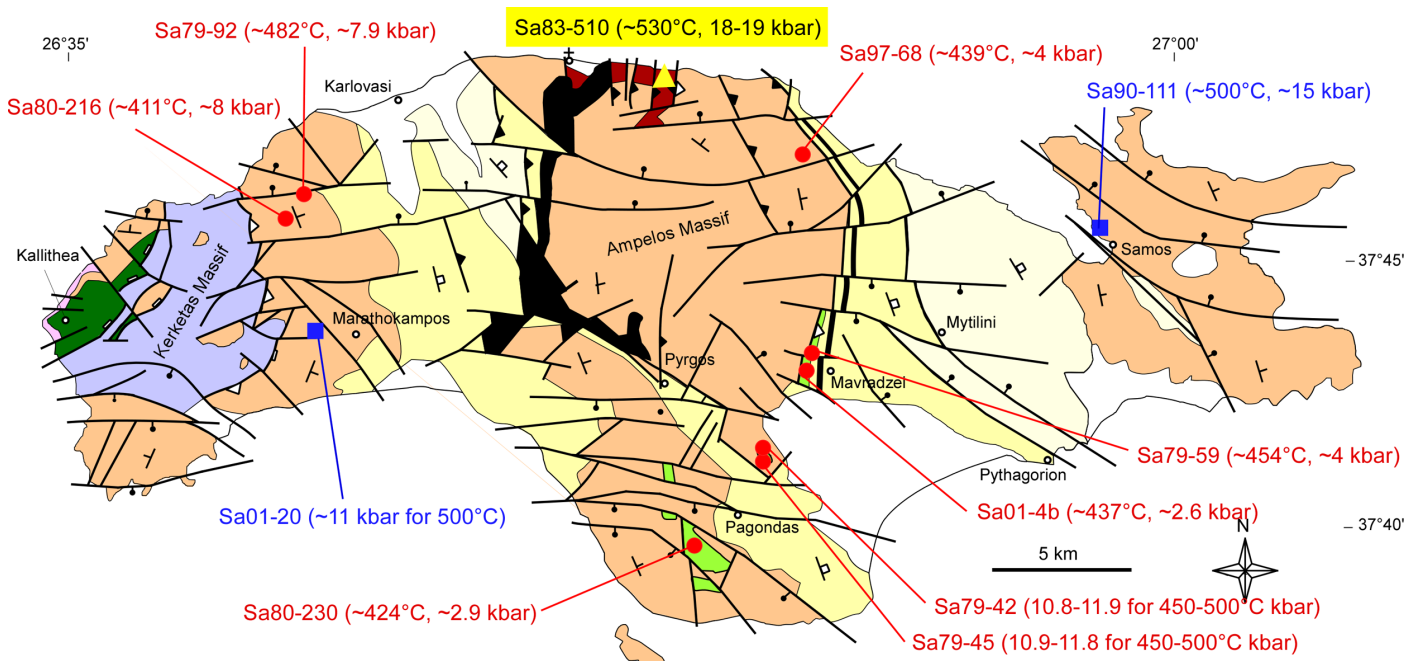


Assemblage garnet + glaucophane + epidote + chlorite + phengite + quartz in blueschist; garnet is rotated. Sample Sa80-154, road near Ampelos, central Samos (plane-polarized light, width of photo 3 mm).

### **P-T estimates**

Pressure and temperature (P-T) conditions of formation of peak metamorphic parageneses and mylonitic mineral assemblages were calculated using the average PT method of Powell and Holland (1994). For this, an updated version (5/2001 data) of the thermodynamic data set of Holland and Powell (1998) was used. This was augmented by the application of the jadeite-albite-quartz barometer to omphacite-bearing samples. In addition, phase petrological modelling in the basic model system NCFMASH (Na<sub>2</sub>O-CaO-FeO-MgO-Al<sub>2</sub>O<sub>3</sub>-SiO<sub>2</sub>-H<sub>2</sub>O) was successfully applied to some rocks by Will et al. (1998). The data are given in Table 3 and shown in Figure 8.

Figure 8. Map



Map showing P-T estimates for rocks of Agios Nikolaos, Ampelos and Selçuk nappe.

P-T conditions for high-pressure metamorphism (Table 3) reveal mildly blueschist-facies conditions of ~8-10 kbar and 350-400°C in the Kerketas nappe at 24-21 Ma (Ring et al. 2001). Will et al. (1998) showed that the P-T conditions inferred for high-pressure metamorphism in the overlying Agios Nikolaos nappe of the Cycladic blueschist unit are ~18-19 kbar and ~510-530°C. Age data for the Cycladic blueschist unit for a number of islands (e.g. Sifnos, Naxos, Ios, Syros, Tinos, Ikaria) across the entire Aegean are remarkably similar and are interpreted to date the peak of high-pressure metamorphism at 55-50 Ma (Wijbrans et al. 1990; Tomaschek et al. 2003).  $^{40}\text{Ar}/^{39}\text{Ar}$  dating of phengite by Ring and Layer (2003) showed that a similar age range has to be envisaged for the peak of high-pressure metamorphism in the Cycladic blueschist unit on Samos.

The temperatures inferred for the strongly foliated chloritoid-kyanite-white mica schists from the Ampelos nappe are rather consistent with 500-540°C but pressures ranging from c. 15 to 5 kbar. A possible interpretation of these data is that the rocks experienced a near isothermal decompression from eclogite to epidote-amphibolite and greenschist facies conditions related to tectonic extrusion of the Ampelos nappe between 42-32 Ma (Ring et al. 2007).

In metagabbro from the basal Selçuk nappe, calculations were carried out on mineral assemblages containing barroisitic hornblende, epidote/zoisite, plagioclase,

chlorite and  $\pm$  quartz. Clearly, this is an assemblage transitional between the middle/upper greenschist- and lower blueschist-facies. Furthermore, the jadeite-barometer was used for the omphacite-bearing massive metagabbros. A garnet-amphibolite from the Selçuk nappe in western Turkey yielded well-constrained P-T conditions of  $550 \pm 18^\circ\text{C}$  and  $12.4 \pm 1.2$  kbar, which is considered to reflect maximum P-T in the Selçuk nappe. The conditions inferred correspond with estimates on undeformed metagabbros from Samos: 8-12 kbar and 400-500°C and are transitional between epidote-amphibolite and eclogite facies conditions. In contrast, strongly foliated, mylonitized Selçuk nappe metagabbros in the Selçuk normal shear zone consistently yielded P-T values of  $4 \pm 1.5$  kbar and  $450 \pm 40^\circ\text{C}$ . Similar greenschist facies P-T estimates of c. 3-4 kbar and 420-440°C were also obtained for Selçuk nappe metagabbros that occur as lenses in the underlying Ampelos nappe.

Evidence for high-pressure metamorphism in the Selçuk nappe is only preserved in the unfoliated samples, but is not longer present in the mylonitized metagabbros from the Selçuk normal shear zone. Presumably, this is the case because fluid ingress hydrated the mylonitic metagabbros in the Selçuk shear zone and caused retrogression of the rocks under greenschist facies conditions of 3-5 kbar. According to the age data reported in Ring et al. (2007) the

deformation-related greenschist facies overprint in the Selçuk nappe occurred before 32 Ma.

The Eocene eclogite facies metamorphism (10-12 kbar) of the Selçuk nappe was followed by a shearing-related greenschist facies overprint at 3-4 kbar. These data imply that the Selçuk nappe must have been exhumed by c. 20-30 km between the high-pressure metamorphism and the end of the mylonitization event. This decompression was accompanied by only slight to moderate cooling from 500°C to 420-440 °C and is ascribed to Eocene normal shearing in the Selçuk normal shear zone (Ring et al. 2007).

The P-T data reveal a pronounced metamorphic break (up to 10 kbar) towards higher pressures and temperatures between the Kerketas and Agios Nikolaos nappes. An inverse break in metamorphic pressure of c. 3-5 kbar occurs above the Agios Nikolaos nappe.

## Structural History and Deformation/Metamorphism Relationships

Structural and metamorphic analysis (Ring et al. 1999a, 2001, 2007; Ring and Layer 2003) shows that deformation can generally be divided into four main stages:

(1) Eocene and earliest Oligocene ~ESE-WNW-oriented nappe stacking ( $D_1$  and  $D_2$ ) associated with blueschist- and transitional blueschist/greenschist-facies metamorphism ( $M_1$  and  $M_2$ ). Maximum high-pressure assemblages in the Cycladic blueschist unit developed during the first deformational event,  $D_1$ , and are therefore referred to as  $M_1$ . The associated  $S_1$  foliation was porphyroblastically overgrown by glaucophane, chloritoid and kyanite during a static growth event. Internal imbrication of the nappes of the Cycladic blueschist unit under  $M_1$  peak high-pressure metamorphism occurred at ~44-37 Ma and followed and also was followed by high-pressure mineral growth (Ring et al. 1999a; Ring and Layer 2003).  $D_2$  caused emplacement of the Cycladic blueschist unit onto the Kerketas nappe, which started at ~35-30 Ma and eventually caused high-pressure metamorphism in the latter at 24-21 Ma (Ring et al. 2001). Maximum pressure in the Kerketas nappe occurred during the  $D_2$  deformation and therefore the mildly blueschist-facies event in the Kerketas nappe is regarded as  $M_2$ .  $D_2$  thrusting was out-of-sequence and occurred during decompression bringing 18-20 kbar rocks of the Cycladic blueschist unit on top of 8-10 kbar rocks of the Kerketas nappe. During  $D_2$ , the  $M_1$  high-pressure assemblages in the Cycladic blueschist unit were replaced by  $M_2$  transitional blueschist/greenschist facies assemblages.

Data reported by Ring et al. (2007) showed that the deformation-related greenschist facies overprint in the Selçuk normal shear zone at the top of the Selçuk nappe occurred at the same time as the basal nappes of the Cycladic blueschist unit were thrust onto the foreland. As mentioned above, these data constrain that greenschist facies metamorphism in the uppermost Selçuk nappe can generally be grouped into the  $M_2$  event and occurred before 32 Ma.

(2) A subsequent history of Miocene horizontal crustal extension ( $D_3$ ). In the Ampelos nappe there is evidence that  $D_3$  proceeded before and after a greenschist facies metamorphism ( $M_3$ ). This greenschist facies metamorphic overprint was characterized by the prograde formation of garnet and more rarely by biotite in metapelite of the Agios Nikolaos and Ampelos nappes (Chen 1995). Chen (1995) estimated ~6-7 kbar and 450-490°C for  $M_3$  with slightly higher temperatures in the western than in the eastern part of the island. The data show that  $M_3$  occurred during further decompression but increasing temperature. This  $M_3$  greenschist facies event can not be related to the above mentioned >~32 Ma greenschist facies metamorphic event in the uppermost Selçuk nappe and must be a second greenschist facies event that can also be seen as a post high-pressure metamorphic event in the Kerketas nappe (characterized by the reaction diaspore to corundum during increasing temperature and decreasing pressure) and must therefore be younger than 21 Ma. Ductile flow during  $D_3$  was characterized by a high degree of coaxial deformation but in general caused displacement of upper units towards the ENE. Fission-track dating by Stephanie Brichau (Brichau 2004) shows that ductile top-ENE extensional reactivation at the base of the Selçuk nappe occurred in the Early Miocene as indicated by zircon fission track ages of 20-18 Ma. The zircon fission-track ages consistently young northeastward in the direction of hangingwall slip (Kumerics et al. 2005). One zircon fission track age of  $14.1 \pm 0.8$  Ma from a conglomerate at the southern slopes of Kerkis Mountain suggests that the Kerketas extensional system is slightly younger than the extensional fault at the base of the Selçuk nappe. The pattern of fission-track ages indicates that both extensional fault systems are unrelated to each other.

Late-stage  $D_3$  emplacement of the Kallithea nappe had a top-NW/NNW sense of shear (Ring et al. 1999a). Inception of the Kallithea detachment is fairly well dated at ~10 Ma.

(3) A short period of brittle E-W crustal shortening ( $D_4$ ) occurred between  $>8.6$  to  $\sim 9$  Ma.  $D_4$  shortening caused numerous W-vergent folds and reverse faults and only affected the lower sequence of the Neogene sediments below the unconformity.

(4) A phase of N-S-directed normal faulting ( $D_5$ , 8.6 Ma to Recent). A granodiorite dike in the footwall of the Kallithea detachment yielded a zircon fission track age of  $7.3 \pm 0.6$  Ma (Brichau 2004) indicating that the Kallithea detachment continued to operate or was reactivated during  $D_5$  extension.

The cause for the short-lived  $D_4$  shortening event between 8.6 and 9 Ma remains enigmatic. It is also not fully clear whether E-W shortening during  $D_4$  was coeval with N-S extension; however, the general absence of NW-striking sinistral and NE-striking dextral strike-slip faults suggests that E-W shortening was not coeval with N-S extension. However, it might be that the extensional emplacement of the Kallithea nappe continued during the short-lived shortening event.

## Geomorphology and Holocene Uplift of Northwestern Samos

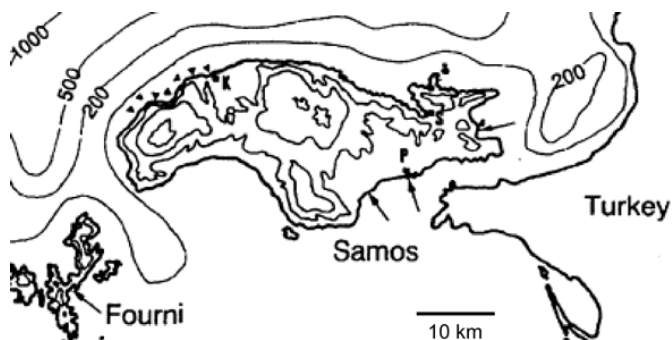
In the past Samos was connected to Anatolia. The narrow strait that is now separating Samos from western Anatolia is less than 1.5 km wide and less than 30 m deep. The coasts in the wider region are characterized by submerged ancient ruins (Flemming 1978), indicating that, at least in the Late Holocene, its coastal morphology is controlled by marine transgression.

Samos is made up by three metamorphic massifs coinciding with topographic highs: the Kerketas Massif in the west, the Ampelos Massif in the central part of the island and the morphologically much less expressed Zoodochos Massif in the east (Fig. 2). These three topographic highs are separated by Neogene sedimentary basins coinciding with topographic lows: the Mytilini basin in the east, the Pyrgos basin in the central part of the island and the Karlovasi basin in the west (Fig. 2). The northwestern part of the island (the northwestern Kerketas Massif) is mountainous and characterized by steep cliffs and highly incised streams with fluvial terraces. The topographic gradient is very pronounced and the coast lines are commonly fault controlled. The topographic gradient decreases markedly to the E and SE. At the SE coast of Samos there is archaeological evidence of coastal subsidence. These relationships

strongly support the interpretation that Samos Island is a tilted horst block.

A more than 1000 m deep marine basin occurs on the northwestern side of Samos (Fig. 9). The bathymetric gradient and the spatial relationship between the deep basin and the pronounced topographic gradient on-land suggest that a major normal fault controls the NW and W coast of the island (Mascle and Martin 1990). The prominent topographic gradient, deeply incised V-shaped valleys with rapids, waterfalls and active pools in the river beds testify to a young, tectonically-controlled relief in the NW. All along the other coasts, the bathymetric gradient is much less pronounced and water depths do not exceed 50-200 m (Fig. 9).

**Figure 9. Uplifted shorelines**



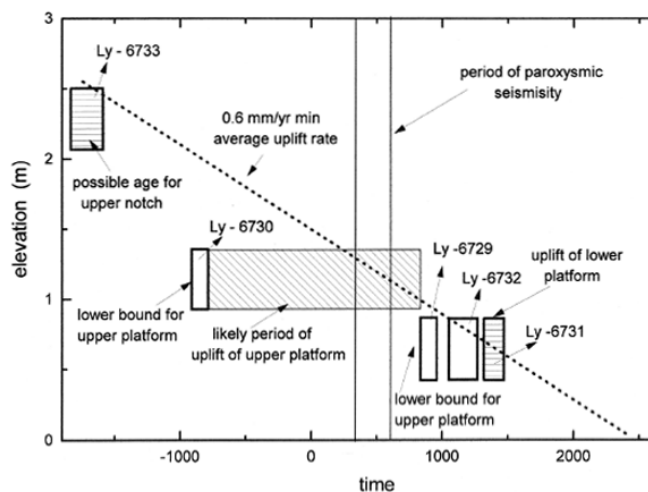
Uplifted shorelines of NW Samos (marked by solid triangles), submerged beaches of SE Samos (marked by arrows) and simplified bathymetry.

Relicts of 3 fossil shorelines and uplifted marine platforms can be found in the northwestern part of Samos (Fig. 9) (they are referred to from top to bottom as the upper notch, the upper platform and lower platform; Stiros et al. 2000). Stiros et al. (2000) interpreted the more or less linear array of uplifted shorelines as being related to Holocene fault activity (see field trip stops #2.1-2.4 below). The fossil shorelines can be traced along a distance of over 10 km along the NW coast of Samos between the Karlovasi harbour and Katavasi Cape and are on average  $0.6 \pm 0.2$ ,  $1.1 \pm 0.2$  and  $2.3 \pm 0.2$  m above sea level. Stiros et al. (2000) showed that the uplifted shorelines are related to earthquakes, which occurred at approximately 500 yr BP (or  $\sim 1500$  AD),  $\sim 1500$  yr BP ( $\sim 500$  AD) and 3600-3900 yr BP (1600-1900 BC). During the punctuated uplifts of the shorelines in a relatively short time interval between 2000 BC and 1500 AD no significant global or regional relative sea-level fall is reported (Pirazzoli 1991), lending further

support into the interpretation that the uplift of the shorelines is tectonically controlled. As argued by Stiros et al. (2000), the preservation of fossil isolated species of the infra-littoral zone (*Vermetus triqueteur*, *Serpulorbis*) on raised shorelines suggests that these species crossed the mid-littoral zone, which is a zone of intense bioerosion, quickly. This indicates a rather rapid and sudden drop in sea level. If the rate of uplift had been slow ( $< \sim 0.5$  mm/yr), the fragile fossil remains would be altered and destroyed in a few years by mid-littoral bioerosion, which is generally considered to proceed at a rate of  $>1$  mm/yr (Torunski 1979).

Stiros et al. (2000) plotted radiocarbon ages against the elevation of the samples from which the radiocarbon ages have been obtained (Fig. 10). The data combine to a loosely defined uplift rate of northwestern Samos of  $\sim 0.6$  mm/yr.

**Figure 10. Radiocarbon ages versus elevation**



Radiocarbon ages versus elevation of samples from uplifted palaeo shorelines and marine platforms from Samos (from Stiros et al. 2000). Boxes indicate the radiocarbon age and elevation uncertainties of the samples analyzed. The horizontal box with thin lines and shading indicates the interval during which the upper platform was fossilized. The average uplift rate defined by the upper notch and the lower platform crosses the rectangle of the likely period of upper platform, at an interval coinciding with the period of paroxysmic seismicity in the Eastern Mediterranean (bounded by the two vertical lines).

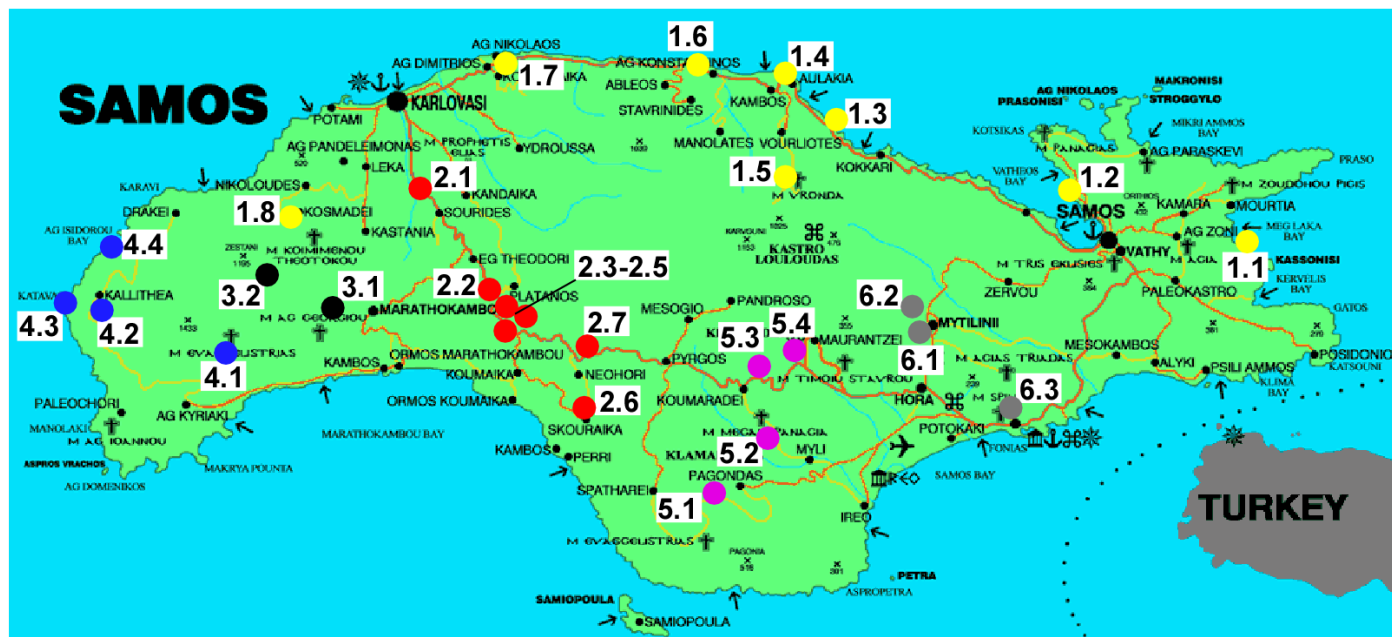
A number of earthquakes of magnitude  $>6$  have been reported from Samos in the last 200 years (at least 6 earthquakes during the 19th century, and another two earthquakes in the 20th century, i.e. 1904  $M=6.8$  and 1955  $M=6.9$ ), but the pre-19th century seismicity remains less well known. In the last 2000 years there is evidence of only 3 well defined earthquakes at  $\sim 200$  BC, at 47 AD and at 1751 AD (Guidoboni et al. 1994; Stiros 1995; Papazachos and Papazachou 1997). There is also some evidence for an earthquake in 1476 AD that devastated Samos and was supposed to be one of the reasons which forced the Genoese, at this time the rulers of the island, and most of the inhabitants to abandon the island and emigrate to nearby Chios Island (Noos 1976).

Stiros et al. (2000) correlated the uplifted shorelines and marine platforms with the seismic events. They concluded that the lower platform, which they dated with radiocarbon at 1306-1467 AD correlates well with the possible earthquake at 1476 AD. The uplift of the middle palaeo shoreline (upper platform in Fig. 10) may correlate with the 47 AD event. However, Stiros et al. (2000) further argue that the seismic uplift occurred at a later period, at  $\sim 500$  AD. Interestingly, this period is broadly consistent with a period during which a series of 4th to 6th century coastal uplifts of unprecedented scale have been identified in the Eastern Mediterranean (Pirazzoli et al. 1996).

## Field Trips

Samos is a fairly large island and good outcrops are sometimes hard to get to. The road system improved considerably over the last decade. The locations of the stops are shown on the simplified road map in Figure 11. We arranged the stops based on infrastructural and geographic constraints and not by geologic themes. The last time we visited Samos was in September 2001 and due to considerable efforts in improving the roads and building tourist facilities things may have changed since then. The field trips start from Samos town, which is the main town on Samos. The best road map is from ROAD Editions.

Figure 11. Road Map



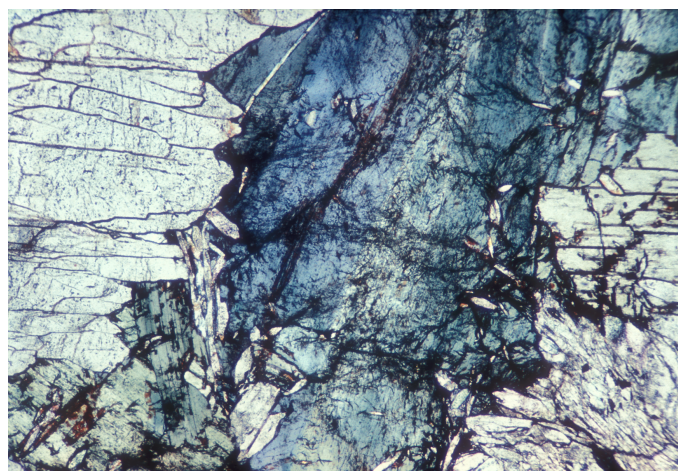
Simplified road map of Samos with locations of stops.

### **Day 1: Metamorphosed rocks of the Ampelos and Agios Nikolaos nappe and Neogene sediments of Mytilini basin in East and North Samos**

#### **Stop #1.1: Mikri Lakka Bay**

The first stop is an abandoned diasporite mine in eastern Samos. Drive from Samos town to the ENE (Kamara, Profitis Ilias). Just before the road starts to climb up towards Profitis Ilias take a right towards Agia Varvara and Mourtiá. Down near the beach there are stairs going up to the south, follow them and then keep going south until you reach the northern slopes of Mikri Lakka Bay (the hike takes about 20-30 minutes). The abandoned metabauxite mine is in greyish marble of the Ampelos nappe. Metabauxite is relatively common in marble of the Cycladic blueschist unit throughout the Aegean and shows that the marble was periodically above sea level and received sediment from nearby continental sources. The Al-phase in this outcrop is diasporite (Fig. 12) and attests that maximum metamorphic temperatures did not exceed ~470-480°C (Mposkos 1978). In western Samos, corundum is the main Al-phase indicating higher temperature conditions in western Samos.

Figure 12. Metamorphic assemblage



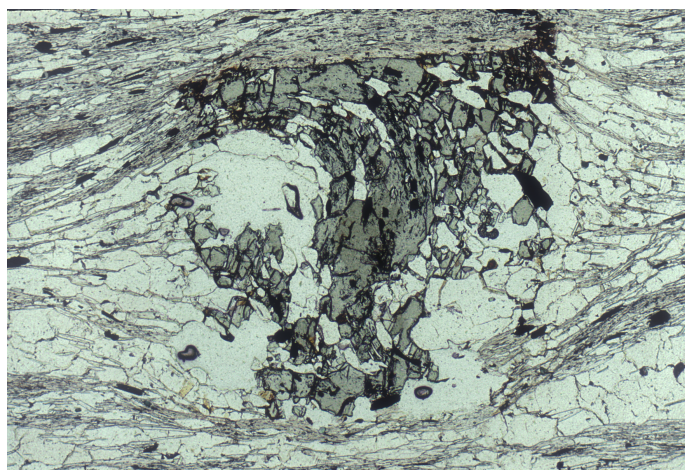
Assemblage diasporite (white) + chloritoid (different shades of blue) in metabauxite; sample Sa80-185 from abandoned diasporite mine, Mikri Lakka Bay, East Samos (plane-polarized light, photo width 4 mm).

#### **Stop #1.2: Gankou Beach (N37°45'59", E26°57'35")**

At the northern end of the small Gankou bay quartzite and quartzitic schist containing several millimeter large chloritoid crystals is exposed. The rocks in the outcrop are characterized by a penetrative  $S_1/S_2$  foliation. An E-W trending stretching lineation, STR1/2, occurs on the foliation planes and this lineation is expressed by stretch quartz-albite aggregates and aligned phengite. Occasionally

small-scale intra-folial folds with axes parallel to STR1/2 can be observed. Thin sections are dominated by the assemblage chloritoid + phengite + quartz (Fig. 13). Chloritoid is commonly rotated. Gessner et al. (this issue) described very nice examples of rotated chloritoid and kyanite from this rock unit in adjacent western Turkey.

**Figure 13. Metamorphic assemblage**



Assemblage chloritoid (light olive green) + phengite + quartz in metapelitic schist; chloritoid is rotated; sample Sa80-222, Gankou Beach, Eastern Samos (plane-polarized light, photo width 3.7 mm).

Ring et al. (2007) dated a mylonitic quartzite from this outcrop, which structurally belongs to the upper contact of the Ampelos nappe and thus is considered part of the Selçuk normal shear zone. Rb-Sr analysis of the minerals that constitute the mylonitic foliation has been hampered by the lack of apatite and problems producing a clean feldspar fraction. Magnetic separation of the white mica populations revealed two chemically distinct white micas. Rock texture suggests that some of these phengite/paragonite intergrowths form textural relics within an otherwise penetratively deformed matrix (see figure 5c in Ring et al. 2007). Rb-Sr data show that there is no age-grain size correlation, which is in line with complete synkinematic recrystallization as inferred from textural observations. Despite evidence for incipient weathering, the whole rock was analyzed as well. Integration of the whole rock data with the different white mica results leads to an apparent deformation age of  $37 \pm 5$  Ma which we interpret as an accurate estimate for late stages of mylonitic deformation.  $^{40}\text{Ar}/^{39}\text{Ar}$  spot-fusion ages show a large variation in ages of  $\sim 10$  Ma. Two pre-mylonitic, non-recrystallized, high-Si phengite/paragonite intergrowths in sample Sa01-1 yielded ages of

$\sim 50$  Ma. The mylonitic phengite yielded no spot-fusion ages  $> \sim 42$  Ma. Analyzed spots from relatively coarse-grained ( $\sim 60$ - $80 \mu\text{m}$ ), early recrystallized phengites in mylonitically sheared layers give systematically older ages than spots from late-stage recrystallized phengites ( $> \sim 50 \mu\text{m}$ ). We interpret the scatter of the ages to be due to progressive recrystallization of phengite. Accordingly we propose that the scatter in ages reflects different increments of shear-zone deformation.

Drive from Samos town towards Kokkari and Karlosvasi. About 2 km west of Samos the road goes through smoothly rolling hills made up primarily by Pliocene porous lacustrine limestone, with subordinate tuffaceous marl and silt of the Kokkari Formation.

### **Stop #1.3: Beaches of Lemonakis and Tsamadou $\sim 2$ km northwest of Kokkari**

Thin-bedded marl of Hora Formation crops out. Towards the top of the exposed section the marls have abundant conglomerate and breccia horizons that signify tectonic uplift related to D<sub>4</sub> shortening.

### **Stop #1.4: West of Avlakia and east of turnoff to Vourliotes**

The view from the road towards the south shows a huge marble sequence of the Ampelos nappe in the west. The relief between the top of the marble and the Neogene sediments of the Mytilini basin to the east is more than 500 m and the structural relief is more than 1000 m.

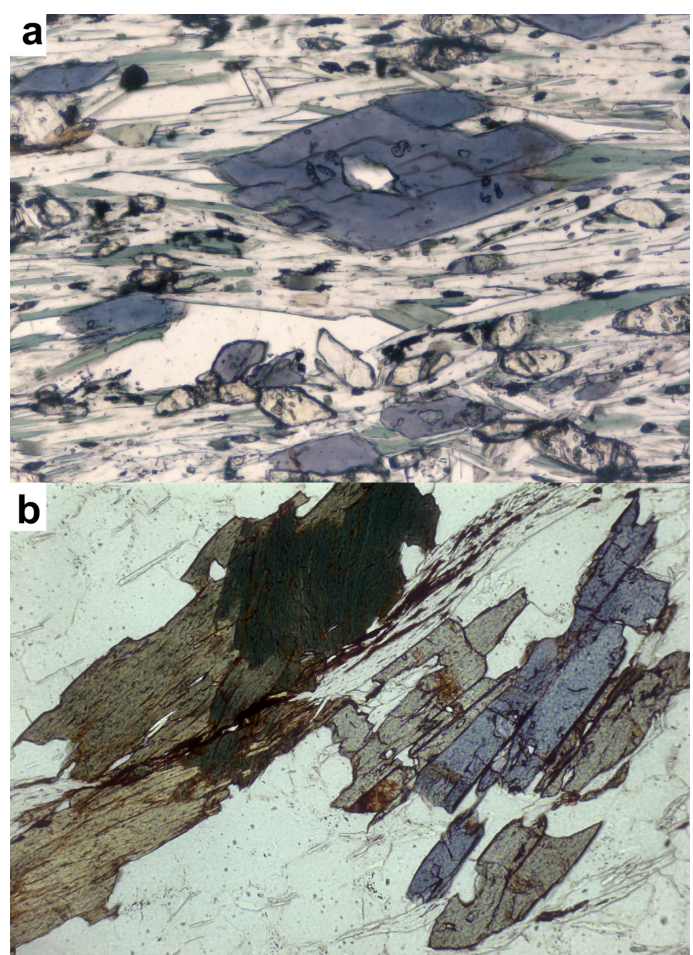
In the road cut a D<sub>4</sub> reverse fault puts marble of the Ampelos nappe above Tortonian marl of the Hora Formation. The fault dips WSW and the shortening direction is WSW-ENE. The sedimentary material is in part silicified; drusy quartz fillings and red iron staining is common in places.

### **Stop #1.5: Monastery Moni Vronda south of Vourliotes**

Less than 1 km west of Stop #1.3 there is a turnoff to the south to Vourliotes. The road climbs up in marble of the Ampelos nappe. In Vourliotes turn left to the monastery of Moni Vronda. Just before you reach the monastery you will find glaucophane-bearing chlorite-rich schists in a little forest to the left of the road. The glaucophane needles are in part well oriented in a NW direction and in part grew randomly on the foliation planes. In thin sections the assemblage glaucophane + epidote + chlorite + phengite + quartz is common in metapelitic schist (Fig. 14a). Further ahead on the right-hand side of the road opposite of the

monastery chloritoid-bearing metapelitic schist is exposed (Fig. 14b).

**Figure 14. Metamorphic assemblages**

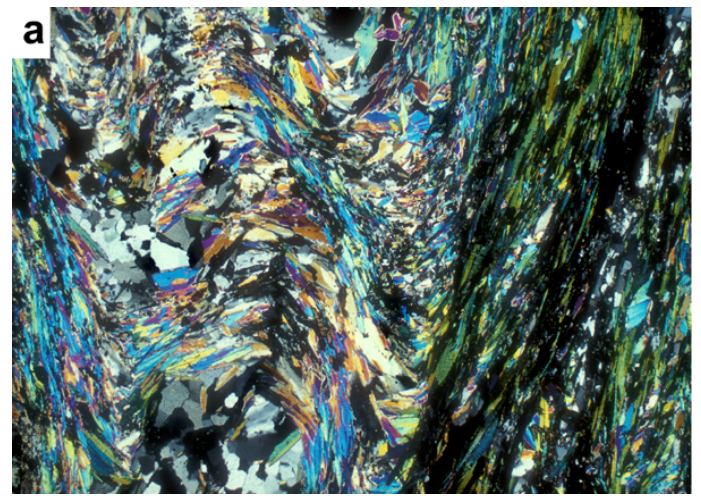


(a) Assemblage zoned glaucophane (blue) + epidote (yellowish grey) + chlorite (green) + phengite + quartz in metapelitic schist from sample Sa79-74, Moni Vronda, central Samos (plane-polarized light, photo width 0.15 mm). (b) Assemblage chloritoid (blue or light olive-green) + chlorite (yellowish green to dark green) + phengite + quartz in metapelitic schist from sample Sa80-190, Moni Vronda, central Samos (plane-polarized light, photo width 1.4 mm).

**Stop #1.6: Around Agios Konstandinos**

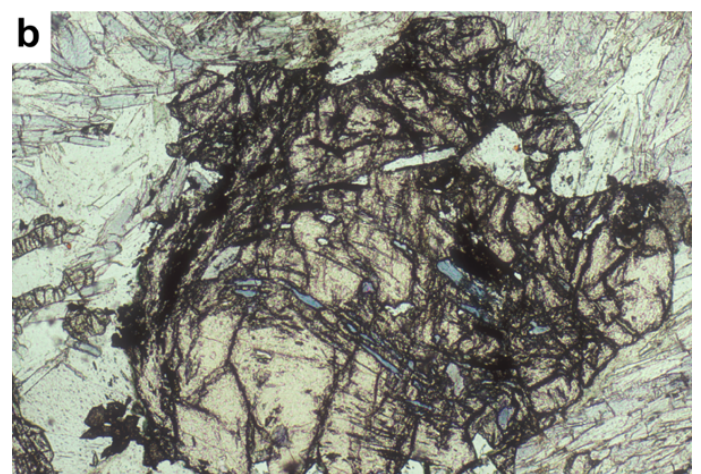
Garnet-mica schist and garnet glaucophanite of the Agios Nikolaos nappe are exposed in a road section. Both rock types preserve excellent high-pressure parageneses (Fig. 15). The main foliation in outcrop is considered to be  $S_2$  and started to develop during high-pressure metamorphism and was then retrograded during ongoing deformation as evidenced by chlorite growth in garnet rims. The internal foliation within the garnets is a high-pressure foliation defined by aligned glaucophane (Fig. 15).

**Figure 15a. Metamorphic assemblages**



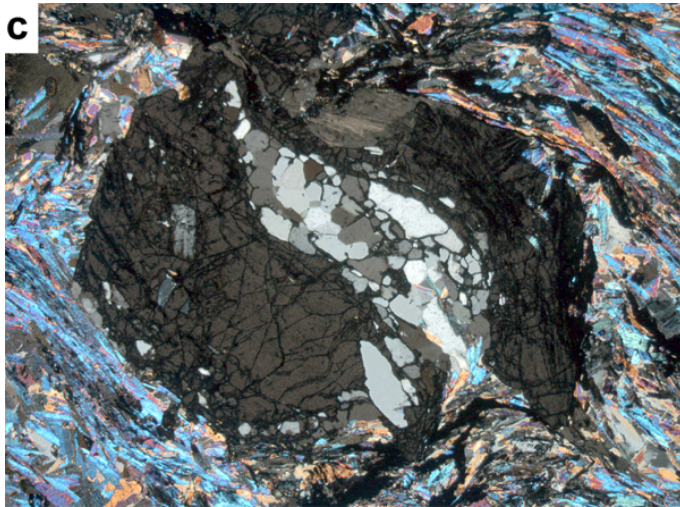
(a) Assemblage phengite + quartz in metapelitic schist, sample Sa83-527, Livadaki E of Agios Konstandinos, north coast of Samos; internal foliation in garnet folded, formation of penetrative  $S_2$  wrapping around garnet (crossed polarized light, photo width 7.8 mm).

**Figure 15b. Metamorphic assemblages**



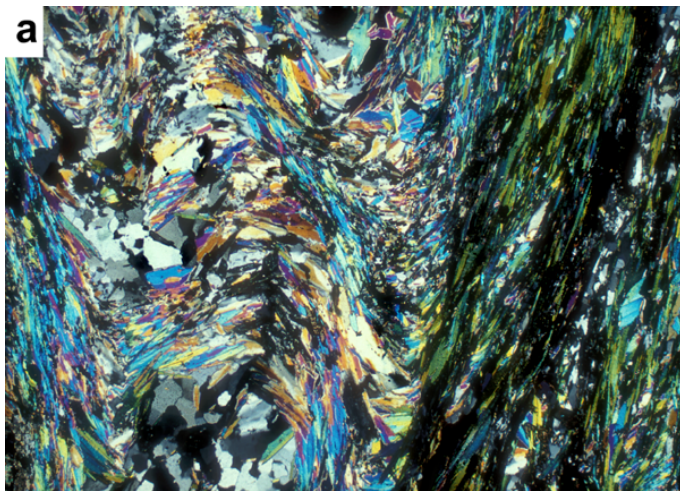
(b) Assemblage garnet (yellow) + glaucophane (light blue) + epidote (yellowish grey) + phengite + quartz + titanite, garnet shows rotated inclusions of glaucophane (darker blue, richer in Fe), sample Sa80-200, Livadaki E of Agios Konstandinos, north coast of Samos (plane-polarized light, photo width 2.4 mm).

**Figure 15c. Metamorphic assemblages**



(c) Assemblage garnet + chloritoid (light green or blue) + chlorite (light green) + phengite + quartz in metapelitic schist, garnet is rotated and partly replaced by chlorite, sample Sa83-514, Livadaki E of Agios Konstandinos, north coast of Samos (plane-polarized light, photo width 4 mm).

**Figure 15d. Metamorphic assemblages**



(d) Garnet + chloritoid + chlorite + phengite + quartz in metapelite, garnet is rotated and partly replaced by chlorite, sample 83-154, Livadaki E of Agios Konstandinos (plane-polarized light, photo width is 4 mm).

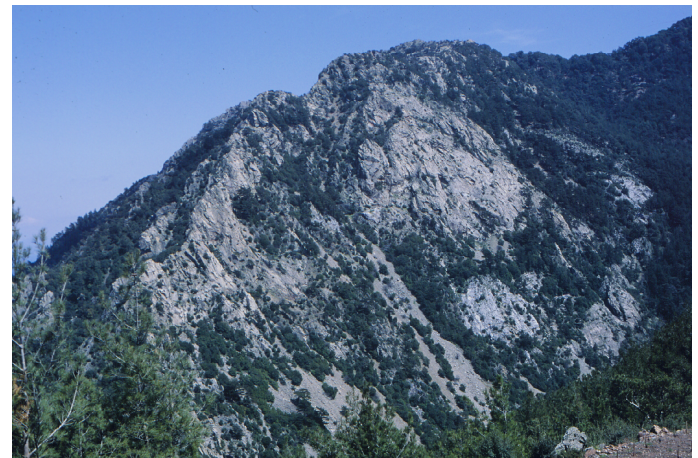
Further west on the northern (beach) side of the road is a house-sized dark-green block of well-foliated garnet glaucophanite. The foliation is defined by aligned glaucophane and formed during high-pressure conditions. There is abundant evidence for quartz/calcite-filled veins. Sample 83-510 yielded the highest pressure recorded on Samos and

Will et al. (1998) reported P-T conditions of ~18-19 kbar and ~530°C.

**Stop #1.7: West of Agios Nikolaos**

Along the road rocks of the Agios Nikolaos nappe are intruded by trachyte. Further south the trachyte also intrudes rocks of the overlying Ampelos nappe. The greyish trachyte forms spectacular cliffs, a few hundreds of meters high (Fig. 16) and in part shows nice alkali-feldspar crystals.

**Figure 16. Landscape**



Spectacular cliffs made up by trachyte.

**Stop #1.8: Kosmadei**

The road to Kosmadei is quite long and winding, so the drive from Karlovasi to Kosmadei might take more than 30 minutes. In the village, especially in the southern and southwestern parts of the village, dark-green, coarse-grained, glaucophane-bearing metagabbro is exposed. Our tectonic interpretation is that the metagabbro represents slices of the Selçuk nappe within the Ampelos nappe.

The metagabbro is usually a fairly massive, dark-green rock containing barroisitic amphibole and in part omphacitic pyroxene. A sample from Kosmadei yield a pressure of ~8 kbar and a temperature of ~410°C (Table 3).

**Overnight in Karlovasi.**

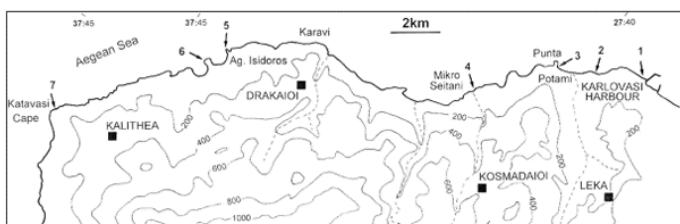
Make own arrangements.

**Day 2: Uplifted shorelines, Neogene sediments and volcanics of the Karlovasi basin and metamorphosed rocks of the Ampelos and nappe in western central Samos**

**Stop #2.1: Karlovasi harbour**

This stop is shown as site 1 in Figure 17. On the rocks directly west of Karlovasi harbour signs of notches, at least 2 m above sea level, though not well developed, can be observed all along the coast towards Potami Beach.

**Figure 17. Landscape**



Raised beaches in NW Samos (from Stiros et al. 2000).

**Stop #2.2: St. Nicholas Chapel at Potami Beach (site 2 in Fig. 17)**

On the beach directly east of the white chapel of St. Nicholas at Potami a well preserved colony of vermetids (mainly *Vermetus triqueter*) has built a thin reef capping slabs of beach rock, up to 50 cm above sea level (Fig. 18). These species live in the infra-littoral zone and they do not represent good indicators of sea level. However, as they are confined to the lower part of the beach rock slabs, their upper part is likely to correspond to the sea level of the period they were living. On the nearby rocks, remains of vermetids (colonies of *Dendropoma petraeum* and isolated *Vermetus triqueter*) were found at two distinct levels: on average 0.6 m and 1.1 m above sea level on coastal rocks. Both levels have been interpreted by Stiros et al. (2000) as fossil shorelines.

**Figure 18. Vermetid micro-reef**



Details of the raised vermetid micro-reef capping at about 10.5 m a beachrock slab, on the beach east of the St. Nicholas Chapel. The Vermetid layer consists mostly of *Vermetus triqueter* (photograph from Stiros et al. 2000).

**Stop #2.3: Punta Promontory (site 3 in Fig. 17)**

Along parts of the eastern side of the Punta Promontory, at the western edge of Potami Beach, there is clear geomorphological evidence of at least three fossil shorelines: two benches,  $0.6 \pm 0.2$  m and  $1.1 \pm 0.2$  m above sea level, and a narrow notch at a height of  $2.3 \pm 0.2$  m (Fig. 19). The lithology is non-uniform even at the scale of a few meters, so these features disappear at the tip of the cape, but reappear on the coast west of the promontory.

**Figure 19. Raised shorelines**



Raised shorelines at Punta. The feet of the person are on the two low benches (about 0.6 and 1.1 m in altitude) and his head is at the elevation of the upper notch (~2.3 m above sea level) (photograph from Stiros et al. 2000).

No biological traces have been found on the two benches, but remains of two polystromatic colonies of *Dendropoma petraeum*, 0.7±0.2 m and 1.1±0.2 m above sea level, respectively, have been found at the eastern edge of the Punta Promontory. These two colonies are interpreted to correspond to two fossil shorelines, geomorphological evidence of which consists of the two adjacent benches.

**Stop #2.4: Mikro Seitani Cove (site 4 in Fig. 17)**

In this outcrop two benches are at a slightly higher (about 20-30 cm) level, probably due to higher wave energy. The 1.5 m high platform looks like a former surf bench, locally more than 1 m wide, and forms an arch at the cape of the eastern edge of the cove (Fig. 20). The corresponding sea level in such a case should be identified at a level of at least 20±30 cm lower than the bench rims (Pirazzoli 1996). The upper notch, although not well developed, is also discernible at ~2.4±0.2 m above sea level (Fig. 20).

**Figure 20. Three fossil Holocene raised beaches**



Mikro Seitani cove showing two coastal platforms and a notch above them testifying to the three fossil Holocene raised beaches (photograph from Stiros et al. 2000).

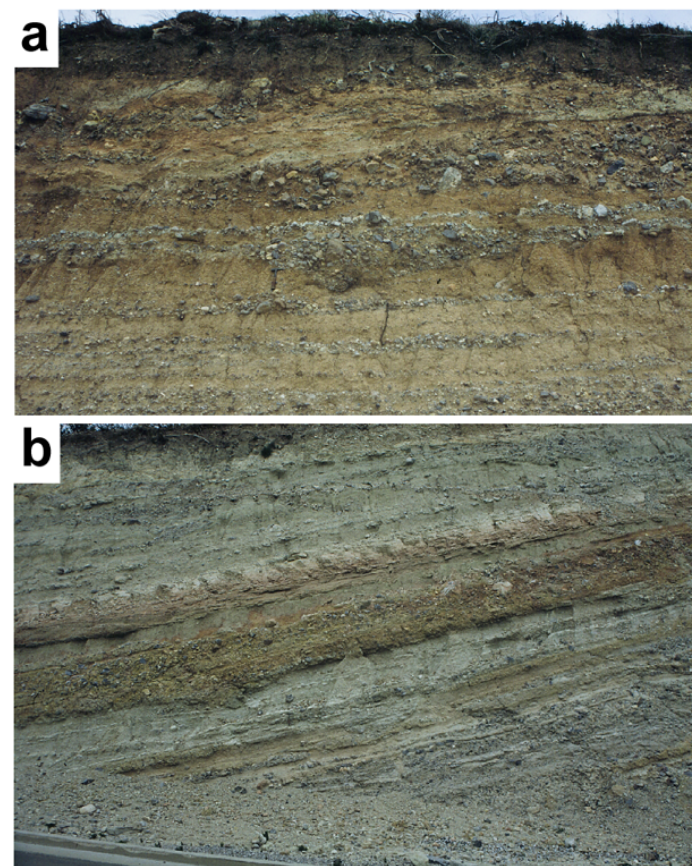
**Stop #2.5: Marl of Hora Formation**

Take the main road to Marathokambos, which climbs smoothly up through marl of the Hora Formation. The thinly bedded marl is exposed in many road cuts. The marl frequently shows slumps and other features of soft-sediment deformation and was deposited in a relatively deep lacustrine environment.

**Stop #2.6: Conglomerate of Mytilini Formation just northwest of turnoff to Platanos**

Reddish conglomerate is exposed on the northern side of the road (Fig. 21). The conglomerate rests above the unconformity in the basin succession. The unconformity and the fluvial depositional environment of the conglomerate is the consequence of the short-lived D<sub>4</sub> shortening event that caused uplift of the region. The uppermost beds of the Mytilini Formation are tuffaceous sands and marls signifying a change from fluvial to lacustrine deposition due to subsidence related to D<sub>5</sub> normal faulting.

**Figure 21. Platanos conglomerates**



(a) Conglomerates near turnoff to Platanos; grain size gets larger towards top of outcrop. (b) Section below that shown in (a) depicting more marl horizons.

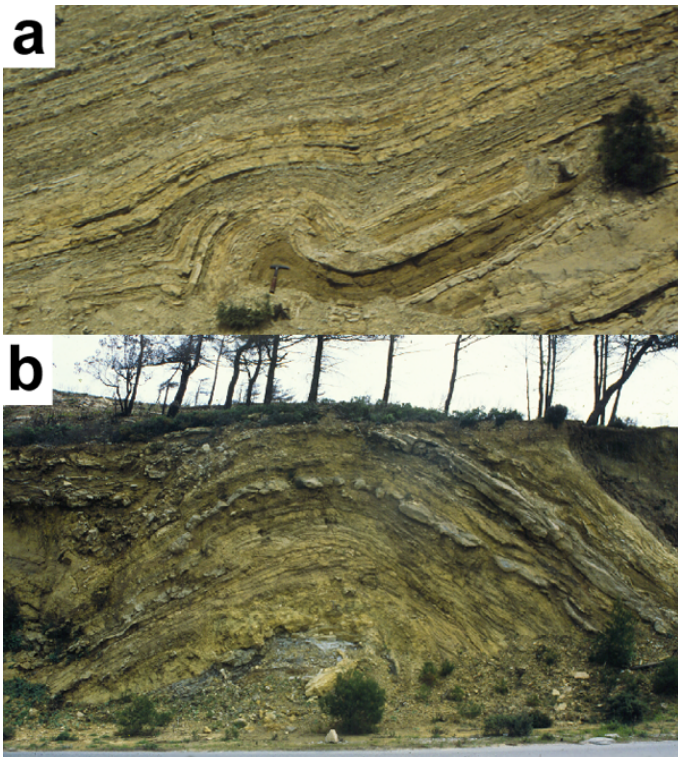
There are abundant rhyolite clasts in the conglomerate indicating that the rhyolite is older than ~9 Ma. Furthermore, abundant metamorphic rocks can be found in the conglomerate.

Stroll a few hundred meters downhill along the road to the east. Thinly bedded marl of the upper Mytilini Formation is exposed. The entire section is dipping to the NW.

### Stop #2.7: Slump folds in marl of the Hora Formation

Walk another ~500-1000 m to the SE along the road you find slump folds in marl (Fig. 22a). The marl is thinly bedded and commonly shows evidence for soft-sediment deformation. In a large road cut on the NE side of the road the slump folds are folded by upright  $D_4$  folds (Fig. 22b). The harder carbonate layers are frequently boudinaged in the limbs of the folds.

Figure 22. Folds



(a) Slump folds in marl; marl in outcrop is thinly bedded; horizons characterized by slumping are restricted to a few layers in marl. (b) Upright  $D_4$  fold in marl folding slump folds; good example can be seen in right limb of fold.

### Stop #2.8: Volcanic rocks at turnoff to Koumeika

Drive a few hundred meters to the SE through pyroclastic rocks until you reach the turnoff to Koumeika. Walk up the gully opposite the turnoff to Koumeika. Greyish dacite with feldspar and hornblende phenocrysts are exposed. Further up to the NE dark basalt is exposed. Occasionally pyroxene and biotite crystals can be found.

The volcanic rocks intruded at the boundary between the Neogene sediments and pyroclastic rocks of the Karlovasi basin and marble of the Ampelos nappe to the E. The marble crops out along the road to Pyrgos to the E of the Koumeika turnoff.

### Stop #2.9: Thick-bedded, travertine-like limestone of the Pythagorion Formation

Follow the road to Koumeika. In road cuts just south of the turnoff thick-bedded, greyish-yellowish-white limestone of the Pythagorion Formation crops out. The limestone was deposited in a shallow lacustrine environment. Freshwater gastropods, stromatolites and onkolites occur and dessication cracks and wave ripples are common. Near the volcanic rocks the limestone is locally strongly silicified. Tuffaceous layers may also occur.

The thick-bedded limestone laterally interfingers with the thin-bedded marl of the Hora Formation, indicating rapid lateral variations in the depositional environment of shallow to relatively deep lacustrine conditions.

A view towards the E shows the limestone in the hills below the main road to Pyrgos and marble of the Ampelos nappe along the road. Both lithologies are separated by a S-dipping  $D_5$  normal fault.

### Stop #2.10: Basal breccia of Basal Conglomerate Formation near Skoureika

In Koumeika turn E to Skoureika. You will drive through gently rolling hills made up by thick-bedded limestone of the Pythagorion Formation. About 500 m W of Skoureika you should start seeing coarse, reddish-brown breccias. The age of the breccia is not known but older than 11.2 Ma. At the base the cobbles are poorly sorted and angular; some boulders may reach 1  $M_3$  in diameter. The pebbles are entirely metamorphic rocks (quartzite, marble and phyllite) (Fig. 23). Cross-bedded sands occur above those cobbles and may have been channel fills of rounded gravels. At the top brown to yellow siltstone with thick palaeosoils frequently cut by gravels occur. Weidmann et al. (1984) interpreted the depositional environment as a proximal to distal floodplain.

**Figure 23. Basal Breccia**



Basal Breccia; the clasts are mainly derived from the nearby metamorphosed nappes.

Weidmann et al. (1984) argued that the pebbles derived from the local basement (Cycladic blueschist unit). This view is in line with the zircon-fission ages of Brichau (2004) yielding ages between 20 and 18 Ma.

#### **Stop #2.11: Glaucophane schist N of Neochori**

Leave Skoureika and turn N to Neochori. Where the road meets the main Pyrgos-Karlovasi road epidote-glaucophane schist is exposed on the northern side of the road. Due to extensive improvement of the road the outcrops have changed considerably in the past years. The well foliated rocks are characterized by large prismatic, dark-blue to black glaucophane reaching 1 cm in length. The glaucophane sits in a yellowish-green matrix made up primarily by epidote with subordinate chlorite.

#### **The best place for staying this night might be Ormos Marathokambos.**

Make own arrangements.

### **Day 3: Triassic granite and traverse from Ampelos into Kerketas nappe**

#### **Stop #3.1: Triassic granite W of Marathokambos**

In the southwestern corner of Marathokambos turn into a small road that goes off to the west (follow sign to Pythagoras cave). Follow the dirt road for about 1.5 km and then deformed granites are exposed in the cliffs on the right hand side of the road. The granite is strongly foliated and the foliation wraps around feldspar porphyroclasts. Single-zircon dating yielded a Triassic age for the granite (Ring et al. 1999a). Ar-Ar dating of hornblende, biotite and white

mica by Ring and Layer (2003) yielded very complicated Ar-diffusion spectra. The oldest event is seen in the hornblende with an age of up to 220 Ma. The next age seen in all three dated minerals is a ~55-60 Ma age. This is an excess Ar event in hornblende, a plateau age in biotite and a 'highest temperature age' in white mica. Both biotite and white mica also show evidence for a 20-25 Ma event. This event is reasonably well recorded in the white mica at  $25.5 \pm 1.7$  Ma, which is probably the best representation of that event. In white mica, an 'intermediate' age at  $37.4 \pm 1.1$  Ma is represented as a fairly well-defined plateau.

If you follow the road for another 1-2 km you will reach dolomite of the Kerketas nappe after a hairpin in the road. Up the cliff to the west is a cave. Legend has it that Pythagoras lived in that cave for a while. The cave is in dolomite of the Kerketas nappe, which is in high-angle fault contact with the Ampelos nappe here. However, to the N this contact is well exposed on a ridge.

#### **Stop #3.2: Traverse from Ampelos into Kerketas nappe (Fig. 24)**

From Pythagoras cave either follow the road to the southern coast or turn round and go back to Marathokambos; 1 km NE of Marathokambos take the road to Kastania and after about 100 m turn left and take a dirt road to the windmills – there are a bunch of modern windmills and some ruins of old windmills. Carry on for about 5-6 km up the hill until you reach the top of a saddle from where the road drops down to the N – park your car here and follow a goat track to the west. You will walk through a generally moderately E-dipping variegated sequence of phyllite (in part carbon bearing and thus dark grey to black), marble, greenschist, chlorite-rich schist and quartzite. Most rocks are strongly foliated and have a WNW-trending stretching lineation. After about 1 km you will reach the greyish-white dolomites of the Kerketas nappe. Directly at the contact a dolomite slice occurs in the phyllite. The contact zone is well exposed but no distinct mylonitic shear zone has been mapped. Instead it appears that the relatively strong deformation recorded in the Ampelos nappe rocks on the ridge took up the deformation heterogeneously. The dolomite of the Kerketas nappe appears hardly deformed at all.

**Figure 24. Panoramic view of contact**



Panoramic view of contact between Ampelos nappe to right and light-grey, dolomitic marble of Kerketas nappe to left; schists of Ampelos nappe are usually covered by greenish-brown vegetation, whereas dolomite commonly has no vegetation, sequence dips to E (i.e. right).

Matthias Bernet measured quartz-c-axis fabrics from quartzites along the contact zone and 8 out of 9 samples yielded an asymmetric fabric indicating a top-ESE shear sense. One single zircon fission-track age of  $14.1 \pm 1.2$  Ma from a metamorphosed conglomerate at the southern slope of the Kerketas nappe (Stop #4.1) is about the same age as the supposed age of the breccia at the base of the Neogene sequence of the Karlovasi basin. Because the closure temperature for fission track in zircon is about the same as the lower limit of quartz ductility ( $\sim 280^\circ\text{C}$ ), the top-ESE shear sense might be Middle Miocene in age and related to extensional reactivation of the Kerketas/Ampelos nappe contact and formation of the Neogene basins on Samos Island. Note that the reasoning is somewhat circumstantial.

If you enjoy hiking you may find your way up to the top of Kerkis Mountain. Towards the top you will probably walk through a variegated sequence of Ampelos nappe rocks again with in part large and beautiful glaucophane crystals (however, that depends on which route you choose in this rugged terrain).

#### ***Spend night again in Ormos Marathokambos.***

Make own arrangements.

#### ***Day 4: Kerketas and Kallithea nappe***

##### ***Stop #4.1: Kerketas nappe at Monastery Evangelistria***

Drive past Votsolakia and then turn to the N; the footpath to Monastery Evangelistria should be signposted. Have a quick stop at the turnoff and look at the impressive

mountainous massif of Kerkis. The monotonous dolomite is exposed (on the northern side of the Kerketas Massif) from the top of the massif all the way down to sea level and the only unit in the central Aegean that compares lithologically to the Kerketas nappe is the Almyropotamos nappe of Evia. Both nappes experienced a poorly defined high-pressure metamorphism ( $\sim 8$ - $10$  kbar and  $350$ - $400^\circ\text{C}$ ) in the Early Miocene at  $24$ - $21$  Ma (Ring et al. 2001; Ring and Reischmann 2002, Ring and Layer 2003).

Follow the dirt road until you reach the path and walk up the hill. After a while you will reach the contact between the Ampelos and Kerketas nappes again, which here is a subvertical brittle fault. A  $\sim 1$  m thick fault zone is exposed in the footpath and the sense of displacement is S-side down.

Carry on along the path to the monastery. Just below the monastery metamorphosed conglomerates are exposed. These conglomerates yielded the zircon fission-track age of  $14.1 \pm 1.2$  Ma (see Stop #3.2). The mean extension direction of the clasts is towards  $70^\circ$ . We also performed an  $R_f/\phi$  analysis which yielded slightly prolate strain geometry. Axial ratios in the XZ plane range from 3.1-8.3.

You might climb further up beyond the monastery and reach the peak of Kerkis Mountain from the southern side. The hike is certainly worthwhile to do and also gives you an impression of the sheer thickness of the monotonous dolomite of the Kerketas nappe. The views from the top are great.

##### ***Stop #4.2: Radiolarite of Kallithea nappe S of Kallithea***

When you drive towards the N to Kallithea you will see the rugged cliffs made up by the dolomite of the Kerketas nappe to your right (Fig. 25). The dolomite also occurs as slices and blocks within the Kallithea nappe (Fig. 5).

**Figure 25. Panoramic view of Kallithea nappe**



Another panoramic view of Kallithea nappe (covered in forest) and light grey dolomite of underlying Kerketas nappe; note that Kerketas dolomite also occurs as blocks and slices within Kallithea nappe; view from the N.

About 500 m S of Kallithea to the W of a 90° curve in the road brownish-red radiolarite of the Kallithea nappe is exposed in the road cut. The radiolarite is in fault contact with basalt and altered peridotite. The radiolarite is well-bedded on the cm scale and bedding is fairly steep in the outcrop. The basalt may show well-preserved pillow structures but is commonly strongly cataclastically deformed. Near faults the basalt becomes green due to hydrothermal alteration.

Stroll around the next bend in the road towards Kallithea and after ~100 m or so you will be in fine-grained whitish to grey limestone of the Kallithea nappe. Bedding is only occasionally discernible as a layering on the dm scale. Try to find *Megalodon*, which may be as large as 10-12 cm (Theodopolous 1979) and indicates a Late Triassic age. Furthermore, lamellibranchiata and gastropods can be found; Theodopolous (1979) reports ostracodes, radiolaria and Jurassic Valvulinidae based on thin-section observations.

#### **Stop #4.3: Tectonic contacts W of Kallithea**

It is quite tricky to find the right turnoffs. Find a dirt road just to the S of Kallithea and follow that road downhill. Bear right initially, then you will come to a curve bending left and you need to take the road to the S here (the one that continues going downhill), take another left at the next intersection.

Once you reach light grey dolomites you are in the Katavasis complex. There is a distinct 10-20 cm thick horizon

of grey to dark grey cataclasite at the top of the dolomite. Now you are where the blue strike and dip sign SW of Kallithea is on the map in Figure 5. You can either hike down a little valley to the beach or continue by car to Katsouni Bay and walk to the N from there. Eventually you will hit a fairly steeply S/SE-dipping sequence of amphibolite and quartzite. The amphibolite crops out on the beach and the quartzite crops out above the amphibolite. Occasionally hornblende crystals in the amphibolite are >1 cm in size. The rocks are metamorphosed at amphibolite-facies conditions. Mezger and Okrusch (1985) speculated that the Katavasis complex belongs to Cretaceous high-temperature rocks, which form crystalline slices within the Cycladic ophiolite nappe on other Aegean islands. The amphibolite and quartzite have a distinct amphibolite-facies foliation and stretching lineation, which is thought to be a relic of the earlier tectonometamorphic history of the Katavasis complex before being emplaced on Samos.

Intruded into this sequence are numerous subvertical, a few decimeter to meter wide granodioritic dikes. One of these dikes yielded an Ar-Ar age of 10.2±0.2 Ma (F. Henjes-Kunst unpubl. data). Stephanie Brichau obtained a zircon fission-track age of 7.3±1.0 Ma from one of the dikes (N37°42'52", E26°34'06").

#### **Stop #4.4: Tectonic contacts N of Kallithea**

Just N of Kallithea there is a turnoff to the left towards Agios Isodoros. The church is in marble and phyllite of the Ampelos nappe. Park the car in the second valley after the turnoff N of Kallithea and make your way down the valley to the sea. Where the creek meets the sea turn to the left and you will find a small slice of Kerketas dolomite tectonically above amphibolite-facies dolomite of the Katavasis complex.

The grey Kerketas dolomite is relatively fine grained and appears hardly deformed in outcrop. In contrast, the underlying dolomite of the Katavasis complex is coarse grained and more whitish in colour. At its top, at the tectonic contact, the Katavasis dolomite is strongly cataclastic and becomes greyish-black in colour. The subhorizontal contact zone is almost knife sharp and very distinct in the field (Fig. 26).

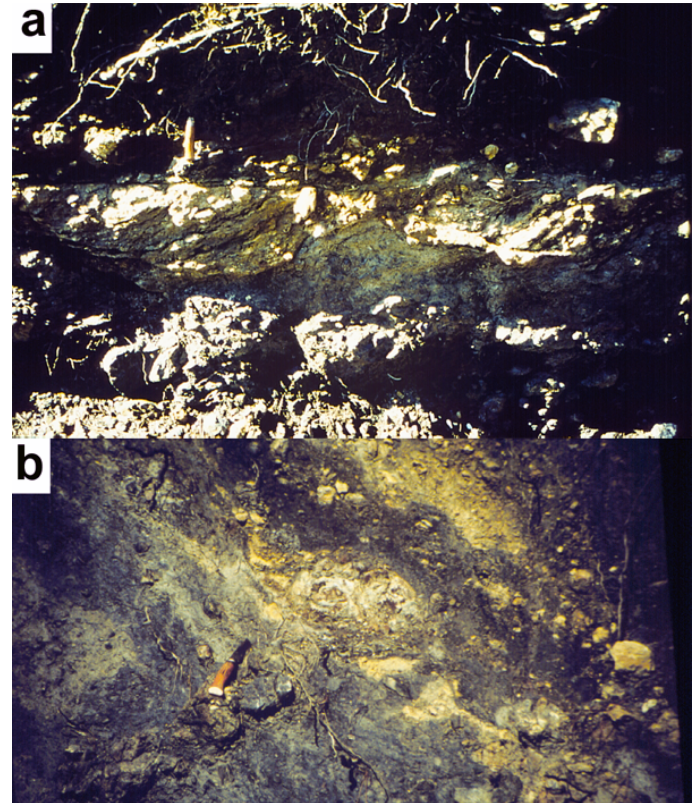
**Figure 26. Nappe contact**



Knife-sharp contact between Kerketas nappe (top) and dolomite of Katavais complex (bottom); dolomite is strongly cataclastically deformed below contact and contains phyllitic lenses.

On the main road from Kallithea towards Drakei, cataclastically deformed pelitic and dolomitic rocks of the Kallithea nappe are exposed in road cuts. Each spring the outcrop situation is different but usually asymmetric brittle structures can be found frequently. Riedel shear and other brittle shear-sense indicators yield top-NW senses of shear (Fig. 27).

**Figure 27. Kerketas nappe**



Brittle deformation in Kerketas nappe (a) Brecciated and cataclastically sheared dolomite layer in shale indicating top-NW (left) shear sense. (b) Strongly cataclastically reworked shale/dolomite sequence.

***Overnight either in Votsolakia or again in Ormos Marathokambos.***

Make own arrangements.

***Day 5: South coast***

***Stop #5.1: Serpentinite-netagabbro profile in road cut between Spatherei and Pagondas***

Drive back up to Marathokambos and take the main road to Pythagorion. In Pyrgos, take a sharp right turn to the S towards Spatherei and Pagondas. About 1 km W of the turnoff to Monastery Evangelistrias a sequence of metagabbro and serpentinite of the Selçuk nappe is exposed. There are numerous steeply dipping faults disrupting the sequence. The metagabbro is usually a massive darkgreen and white rock and does not show much evidence for deformation. However, occasionally flaser gabbro occurs and the spotty green/white appearance gives rise to a foliated

fabric in which greenish and whitish layers alternate. Dark-green serpentinite commonly is well foliated and quite often contains several millimeter big euhedral magnetite crystals.

Metagabbro sample Sa80-230 described in Ring et al. (2007) is from this sequence. The metagabbro is massive and contains omphacite. Furthermore, green and colourless hornblende, diopsidic pyroxene, epidote, chlorite, albite, quartz, and accessory titanite. The metagabbro has a relict magmatic, massive texture: large, anhedral magmatic green hornblende is rimmed by pale green to colourless actinolite and actinolite-chlorite±titanite intergrowths. Magmatic clinopyroxene is rimmed by green hornblende and, in places, replaced by colourless chlorite. Albite both occurs as large poikiloblasts containing fine-grained actinolite, chlorite and epidote, and as fine-grained recrystallized minerals. Compositionally, the amphiboles range from almost pure actinolite to Mg-hornblende. Ca-pyroxene is a diopside-dominated solid solution of 63-75 mole % diopside, 17-21 mole% hedenbergite and 2-10 mole% enstatite. Na-pyroxene has up to 9.5 wt.% Na<sub>2</sub>O and forms a solid solution of 31-52 mole% jadeite, 9-25 mole% acmite, 30-54 mole% diopside and 1-7 mole% hedenbergite.

Drive towards Pagondas, which sits on Neogene basin sediments, and then go towards Ireon. It is worthwhile to visit the temple of Heraion, which was built near the mouth of the river Imvrasos. Only one column of the Heraion temple remained intact (Fig. 28).

**Figure 28. Heraion temple**



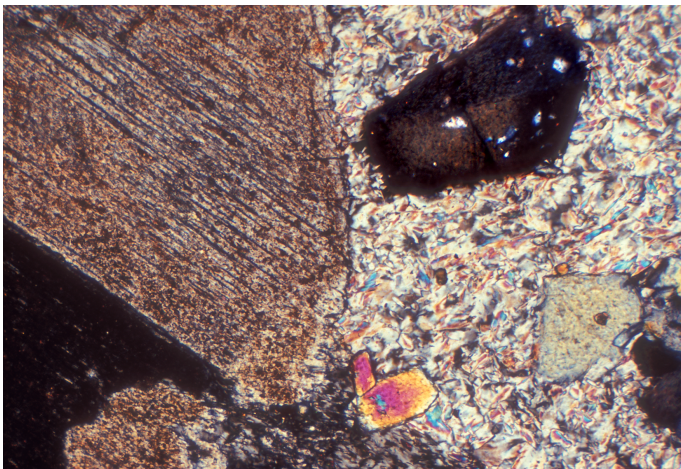
The only surviving column of the Heraion temple constructed in ~530 BC. Displacement of the drums is thought to be due to high seismic accelerations (Stiros 1996), similar to those expected to have been produced by earthquakes responsible for the coastal uplift of the Karlovasi area (photograph from Stiros et al. 2000).

Then head towards Mili and from there to Koumadarei.

#### **Stop #5.2: Road from Mili to Koumadarei**

There is a good mix of almost all rock types of the Ampelos and Selçuk nappe exposed in road cuts. About 1-2 km NW of Mili in a hairpin of the road, weakly deformed metagabbro is exposed. In thin sections, relict magmatic clinopyroxene is common (Fig. 29).

Figure 29. Metagabbro



Metagabbro with relicts of igneous clinopyroxene and porphyroblasts of epidote in a matrix of phengite; sample Sa79-39, crossed-polarized light, photo width 0.9 mm.

Further up the road opposite the turnoff to Monastary Mengali Panagia, strongly deformed chloritoid schist is exposed in the road cut on the left-hand side.

In Koumaradei turn right towards Pythagorion and stop in a hairpin bend about 1 km E of Koumadarei.

**Stop #5.3: View across Mytilini basin and Quarternary plains**

Towards the NE you see Neogene sediments of the Mytilini basin. To the E you look over Quarternary plains on which the airport of Pythagorion was built. In the distance the high mountains of Dilek Peninsula in western Turkey can be seen. Dilek Peninsula is made up of the same rock types as the Aeplos nappe and the Dilek nappe has been correlated to the Ampelos nappe by Ring et al. (1999b).

The road down into the basin is in ordinary Ampelos marble. Near Gionidas take a left towards Mavradzei.

**Stop #5.4: Mavradzei fault zone and gabbros**

The metagabbro is very similar to the one near Pagondas (Stop #5.1); however, in sample Sa79-42 pseudomorphs after lawsonite have been observed (Ring et al. 2007). The metagabbro has been caught-up in the Mavradzei fault zone and therefore has a subvertical foliation and contains numerous small-scale faults. In some of the outcrops decimetre-sized Riedel structures occur.

**Overnight in Ireon or Pythagorion.**

Make own arrangements.

## References

### References

- Brichau, S. 2004. Constraining the tectonic evolution of extensional fault systems in the Cyclades (Greece) using low-temperature thermochronology. Unpublished PhD thesis, Mainz University, Germany.
- Chen, G. 1995. Evolution of the high- and medium-pressure metamorphic rocks on the island of Samos, Greece. *Annales Geologie Pays Hellenic*, 36: 799-915.
- Flemming, N. 1978. Holocene eustatic changes and coastal tectonics in the Northeast Mediterranean: implications for models of crustal consumption. *Trans. R. Soc. London Ser. A*, 289, 405-458.
- Gessner, K., U. Ring, C. W. Passchier, and T. GÜngör. 2001. How to resist subduction: evidence for large-scale out-of-sequence thrusting during Eocene collision in western Turkey. *Journal Geological Society London*, 158: 769-784.
- Godfriaux, I. 1968. Etude géologique de la région de l'Olympe (Grèce). *Annales Géologiques des Pays Helleniques*, 19: 1-271.
- Guidoboni, E., Comastri, A. and Traina, G. 1994. Catalogue of ancient earthquakes in the Mediterranean area up to the 10th century. *Instituto Nazionale di Geofisica, Rome*, 504 pp.
- Holland, T. J. B., and R. Powell. 1998. An internally consistent thermodynamic data set for phases of petrological interest. *Journal Metamorphic Geology*, 16: 309-344
- Kumerics, C., U. Ring, S. Brichau, J. Glodny, and P. Monié. 2005. The extensional Messaria shear zone and associated brittle detachment faults, Aegean Sea, Greece, *Journal Geological Society London*, 162: 701-721.
- Masclé, J. and Martin, L. 1990. Shallow structure and recent evolution of the Aegean Sea: a synthesis based on continuous reflection profiles. *Marine Geology*, 94, 271-299.
- Mezger, K. and Okrusch, M. 1985. Metamorphism of a variegated sequence at Kallithea, Samos, Greece. *Tschermaks Mineralogische Petrographisch Mitteilungen*, 34: 67-82.
- Mposkos, E. 1978. Diasporit- und Smirgelvorkommen der Insel Samos (Griechenland). 4th International congress for the study of bauxites, 2: 614-631.
- Noos, N. 1976. Samos, Our Land, Athens, 176pp (in Greek).
- Okrusch, M. 1981. Chloritoid-führende Paragenesen in Hochdruckgesteinen von Samos. *Fortschritte Mineralogie Beihefte*, 1: 145-146.
- Papazachos, B. and Papazachou, C. 1997. The Earthquakes of Greece, Zitis, Thessaloniki.
- Pirazzoli, P.A. 1991. World Atlas of Holocene Sea-Level Changes. Elsevier Oceanography Series, 58, Amsterdam. 300 p.
- Pirazzoli, P.A. 1996. Sea-level changes: The Last 20,000 Years. Wiley, London, 211 p.
- Pirazzoli, P.A., Laborel, J. and Stiros, S.C. 1996. Coastal indicators of rapid uplift and subsidence: examples from Crete and other Eastern Mediterranean sites. *Zeitschrift Geomorphologie, Suppl.* 102, 21-35.
- Powell, R., and T.J.B. Holland. 1994. Optimal geothermometry and geobarometry. *American Mineralogist*, 79: 120-133.
- Ring, U., S. Laws, and M. Bernet. 1999a, Structural analysis of a complex nappe sequence and late-orogenic basins from the Aegean Island of Samos, Greece. *Journal Structural Geology*, 21: 1575-1601.
- Ring, U., K. Gessner, T. GÜngör, and C. W. Passchier. 1999b. The Menderes belt of western Turkey and the Cycladic belt in the Aegean—do they really correlate? *Journal Geological Society London*, 156: 3-6.
- Ring, U., and Layer, P.W. 2003. High-pressure metamorphism in the Aegean, eastern Mediterranean: Underplating and exhumation from the Late Cretaceous until the Miocene to Recent above the retreating Hellenic subduction zone. *Tectonics*, 22: 1022, 23p.
- Ring, U., P. W. Layer, and T. Reischmann. 2001. Miocene high-pressure metamorphism in the Cyclades and Crete, Aegean Sea, Greece: Evidence for large-magnitude displacement on the Cretan detachment. *Geology*, 29: 395-398.
- Ring, U., and T. Reischmann. 2002. The weak and superfast Cretan detachment, Greece: Exhumation at subduction rates in extrusion wedges. *Journal Geological Society London*, 159: 225-228.
- Ring, U., Will, T., Glodny, J., Kumerics, C., Gessner, K., Thomson, S.N., GÜngör, T., Monie, P., Okrusch, M. & Drüppel, K. (2007): Early exhumation of high-pressure rocks in extrusion wedges: The Cycladic blueschist unit in the eastern Aegean, Greece and Turkey. *Tectonics*, 26, TC2001, doi:10.1029/2005TC001872.
- Stiros, S. 1995. Archaeological evidence of antiseismic constructions in antiquity. *Annaloes Geofisica*, 38, 725-736.
- Stiros, S.C., J. Laborelb, F. Laborel-Deguenb, S. Papageorgiuc, J. Evind, and P.A. Pirazzolie. 2000. Seismic coastal uplift in a region of subsidence: Holocene raised shorelines of Samos Island, Aegean Sea, Greece. *Marine Geology*, 170, 41-58.
- Theodoropoulos, D. 1979. Geological map of Greece, 1:50000, Samos Island: I.G.M.E., Athens.
- Tomaschek, F., A. Kennedy, I. Villa, M. Lagos, and C. Ballhaus. 2003. Zircons from Syros, Cyclades, Greece – recrystallization and mobilization during high pressure metamorphism, *Journal Petrology*, 44: 1977-2002.

Torunski, H. 1979. Biological erosion and its significance for the morphogenesis of limestone coasts and for nearshore sedimentation (Northern Adriatic). *Senckenbergiana maritima*, 11, 193-265.

Weidmann, M., Solounias, N., Drake, R. E. and Curtis, G. H. 1984. Neogene stratigraphy of the eastern basin, Samos island, Greece. *Geobios*, 17: 477-490.

Wijbrans, J. R., M. Schliestedt, and D. York. 1990. Single grain argon laser probe dating of phengites from the blueschist to greenschist transition on Sifnos (Cyclades, Greece), *Contributions Mineralogy Petrology*, 104: 582-593.

Will, T., Okrusch, M., Schmädicke, E., and Chen, G. 1998. Phase relations in the greenschist-blueschist-amphibolite-eclogite facies in the system Na<sub>2</sub>O-CaO-FeO-MgO-Al<sub>2</sub>O<sub>3</sub>-SiO<sub>2</sub>-H<sub>2</sub>O (NCFMASH), with application to metamorphic rocks from Samos, Greece. *Contributions Mineralogy Petrology*, 132, 85-102.

Error: no bibliography entry: d0e971 found in <http://doc-book.sourceforge.net/release/bibliography/bibliography.xml>